

PenPC: A Two-step Approach to Estimate the Skeletons of High Dimensional Directed Acyclic Graphs

Min Jin Ha¹, Wei Sun^{1,2*}, and Jichun Xie³

¹*Department of Biostatistics, University of North Carolina at Chapel
Hill*

²*Department of Genetics, University of North Carolina at Chapel Hill*

³*Department of Statistics, Temple University*

Abstract

Estimation of the skeleton of a directed acyclic graph (DAG) is of great importance for understanding the underlying DAG and causal effects can be assessed from the skeleton when the DAG is not identifiable. We propose a novel method named **PenPC** to estimate the skeleton of a high-dimensional DAG by a two-step approach. We first estimate the non-zero entries of a

*to whom correspondence should be addressed

concentration matrix using penalized regression, and then fix the difference between the concentration matrix and the skeleton by evaluating a set of conditional independence hypotheses. For high dimensional problems where the number of vertices p is in polynomial or exponential scale of sample size n , we study the asymptotic property of **PenPC** on two types of graphs: traditional random graphs where all the vertices have the same expected number of neighbors, and scale-free graphs where a few vertices may have a large number of neighbors. As illustrated by extensive simulations and applications on gene expression data of cancer patients, **PenPC** has higher sensitivity and specificity than the standard-of-the-art method, the PC-stable algorithm.

KEYWORDS: DAG, Penalized regression, log penalty, PC-algorithm, skeleton

1 Introduction

To understand the molecular mechanisms of human disease, huge amount of high-dimensional genomic data have been collected from large number of samples. For example, as of Feb 6th, 2014, The Cancer Genome Atlas (TCGA) project (McLendon et al., 2008) has published multiple types of genomic data in 8,909 cancer patients of 28 cancers. Many statistical methods have been developed to identify the associations between genomic features and disease outcomes or cancer subtypes. However, such association results are descriptive in their nature, and they cannot deliver “actionable” conclusions for cancer treatment. Many recently developed cancer drugs are so-called “targeted drugs” that target particular (mutated) proteins in cancer cells, and the mechanism of such drugs can be understood as direct interventions on tumor cells (Vogelstein et al., 2013). To characterize or predict the consequences

such drug interventions, statical methods that allow causal inference based on high dimensional genomic data are urgently needed.

One of the most commonly used tools for causal inference among a large number of random variables is the directed acyclic graph (DAG) (also known as Bayesian Network) (Lauritzen, 1996; Pearl, 2009). In a DAG, all the edges are directed, and the direction of an edge implies a direct causal relation. There is no loop in a DAG. Such “acyclic” property is necessary to study causal relations (Spirtes et al., 2000). When we remove the directions of all the edges in a DAG, the resulting undirected graph is the *skeleton* of the DAG.

Estimation of the skeleton of a DAG is of great importance. First, it is a crucial step towards estimating the underlying DAG. Second, in many real data analyses where only observational data (instead of interventional data) are available, the DAG is not identifiable but the skeleton can be estimated; and previous studies have shown that causal effects can be assessed from the skeleton of a DAG because a limited number of edges of a DAG skeleton can be oriented using a set of deterministic rules (Maathuis et al., 2009, 2010). Several methods have been developed to estimate DAGs or their skeletons from observational data (Heckerman et al., 1995; Spirtes et al., 2000; Chickering, 2003; Kalisch and Bühlmann, 2007), however most of them are not suitable (theoretically and/or computationally) for the high dimensional genomic problems that motivate our study. For example, in the real data analysis presented in Section 6, we sought to construct DAG of thousands of genes using hundreds of samples. In this paper, we proposed a new method named **PenPC** to address this challenging problem. We proved the estimation consistency of **PenPC** for high dimensional settings of $p = O(\exp\{n^a\})$ for $0 \leq a < 1$, and we also derived

the conditions for estimation consistency for two types of graphs: random graph where all the vertices have the same expected number of neighbors, and scale-free graphs where a few vertices can have much larger number of neighbors than other vertices. As verified by both simulation and real data analyses using TCGA data, **PenPC** provides more accurate estimates of DAG skeletons than existing methods.

The remaining parts of this paper are organized as follows. In Section 2, we give a brief review of DAG estimation methods and the conceptual advantages of our **PenPC** algorithm. Details of the **PenPC** algorithm are introduced in Section 3 and its theoretical properties are presented in Section 4. We study the empirical performance of **PenPC** and existing methods in simulations and real data analyses in Section 5 and Section 6, respectively. Finally, we conclude in Section 7.

2 Review of DAG Estimation

2.1 Directed Acyclic Graph (DAG)

A DAG of random variables X_1, \dots, X_p is a directed graph with no cycle. Specifically, a DAG can be denoted by $\mathcal{G} = (V, E)$, where V contains p vertices $1, 2, \dots, p$ that correspond to X_1, \dots, X_p , and E contains all the directed edges. In a DAG, a *chain* of length n from i to j is a sequence $i = i_0 - i_1 - \dots - i_{n-1} - i_n = j$ of distinct vertices such that $i_{l-1} \rightarrow i_l \in E$ or $i_l \rightarrow i_{l-1} \in E$ for $l = 1, \dots, n$; and a *path* of length n from i to j is a sequence $i = i_0 \rightarrow i_1 \rightarrow \dots \rightarrow i_n = j$ of distinct vertices such that $i_{l-1} \rightarrow i_l \in E$ for $l = 1, \dots, n$. Given this path, i_{l-1} is a *parent* of i_l , i_l is a *child* of i_{l-1} , i_0, i_1, \dots, i_{l-1} are *ancestors* of i_l , and i_{l+1}, \dots, i_n are *descendants* of i_l .

Given a DAG \mathcal{G} for random variables X_1, \dots, X_p and assume that

$$\mathbf{X} = (X_1, \dots, X_p)^T \in \mathbb{R}^p \sim P_X \text{ with density } f_X. \quad (1)$$

We say that the distribution P_X is *Markov* to \mathcal{G} if the joint density f_X satisfies the *recursive factorization*

$$f(x_1, \dots, x_p) = \prod_{i=1}^p f(x_i | x_{\mathbf{pa}_i}), \quad (2)$$

where \mathbf{pa}_i denotes the parents of vertex i . The factorization naturally implies acyclic restriction of the graph structure. Equivalently P_X is Markov to \mathcal{G} if every variable is conditionally independent of its non-descendants given its parents. A related concept is the so-called *faithfulness*:

Definition 1. *Let P_X be Markov to \mathcal{G} . $\langle \mathcal{G}, P_X \rangle$ satisfies the faithfulness condition if and only if every conditional independence relation true in P_X is entailed by the Markov property applied to \mathcal{G} (Spirtes et al., 2000).*

This means that if a distribution P_X is faithful to DAG \mathcal{G} , all conditional independences can be read off from the DAG \mathcal{G} using d-separation defined in the following definition 2, and thus the faithfulness assumption requires stronger relationship between the distribution P_X and the DAG \mathcal{G} than the Markov property.

Definition 2. (*d-separation*). *A vertex set \mathbf{S} block a chain \mathbf{p} if either (i) \mathbf{p} contains at least one arrow-emitting vertex belonging to \mathbf{S} , or (ii) \mathbf{p} contains at least one collision vertex (e.g., j is a collision vertex if the chain includes $i \rightarrow j \leftarrow k$) that is outside \mathbf{S} and no descendant of the collision vertex belongs to \mathbf{S} . If \mathbf{S} blocks all the chains between two sets of random variables X and Y , we say “ \mathbf{S} d-separates X and Y ” (Pearl, 2009).*

Not all the distributions can be faithfully represented by a DAG. In this paper, we assume the random variables follow multivariate normal distribution, then the faithfulness assumption can be justified by the fact that among all the multivariate normal distributions associated with \mathcal{G} , the non-faithful ones form a Lebesgue null set (Meek, 1995).

Given multivariate normal distribution assumption, a commonly used graphical model is Gaussian Graphic Model (GGM), where two vertices are connected if the corresponding two variables are independent, given all the other variables. A GGM can be constructed by a *concentration matrix* (i.e., precision matrix, or inverse of covariance matrix) in that two vertices are connected if the corresponding elements in the concentration matrix is non-zero. The skeleton of a DAG is different from its GGM because of v-structures. In a *v-structure* $X \rightarrow W \leftarrow Z$, co-parent X and Z are marginally independent or conditionally independent given their parents, but given every vertex set that contains W (a collision vertex) or any descendant of W , X and Z are dependent with each other. A few examples are shown in Figure 1, and instances of the covariance and concentration matrices of the GGM in Figure 1(a) are shown in the Supplementary Materials, Section 1.

2.2 DAG estimation using observational data

Many methods have been developed for DAG estimation using interventional data. Since the focus of this paper is DAG skeleton estimation using observational data, we will only provide a brief review for relevant methods using observational data.

When the p variables have a nature ordering (i.e., for any vertex X_i , all the parents or ancestors of X_i are among the vertices X_1, \dots, X_{i-1} , and all the children

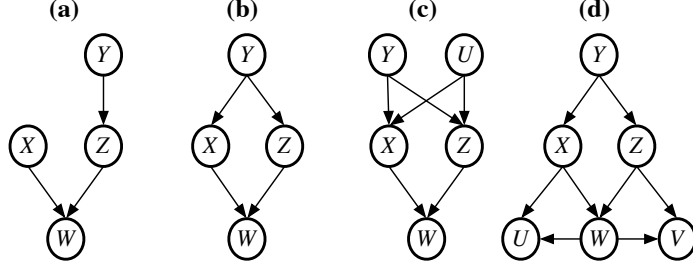


Figure 1: Four DAGs where X and Z are not connected in the skeleton, but are connected in the corresponding GGMs. The true relation between X and Z can be revealed by appropriate conditional independence testing. For example, $X \perp Z$ in Figure 1(a), $X \perp Z|Y$ in Figure 1(b), $X \perp Z|(Y, U)$ in Figure 1(c), and $X \perp Z|Y$ in Figure 1(d).

or descendants of X_i are among vertices X_{i+1}, \dots, X_p), the problem of skeleton estimation is greatly simplified because a regression of X_i versus X_1, \dots, X_{i-1} can be used to identify the true skeleton (Shojaie and Michailidis, 2010). However, in many high-dimensional problems, such a nature ordering is not available. Throughout this paper, we assume no knowledge of nature ordering. Then the underlying DAG is not identifiable from observational data, because conditional dependencies implied by the Markov property on the observational distribution P_X only determine the *skeleton* and *v-structures* of the graph (Pearl, 2009). All the DAGs with the same skeleton and v-structures correspond to the same probability distribution and they form a *Markov equivalence class*. After estimating skeleton, the v-structures can be identified by a set of deterministic rules, and thus we do not distinguish the estimation of a DAG skeleton and a Markov equivalence class.

In general, there are two approaches for DAG or DAG skeleton estimation. The

first one is the search-and-score approach that searches for the DAG that maximizes or minimizes a pre-defined score, such as BIC (Bayesian Information Criterion). The second one is the constraint-based approach that constructs DAGs by assessing conditional independence of random variables. There are also some hybrid methods that combine more than one method.

Direct search across all possible graphs is computationally infeasible even for moderate number of variables. Elegant methods have been developed to search across Markov equivalence classes (Chickering, 2003) or the nature orderings of the variables (Teyssier and Koller, 2005). The objective function of search-and-score methods (e.g., BIC) may be considered a L_0 -penalized likelihood, and a recent work shows several theoretical merits of L_0 -penalized maximum likelihood estimates (van de Geer and Bühlmann, 2013). These methods, however, are still computationally very challenging for genomic applications where the number of vertices can be thousands and sample size ranges from tens to thousands.

One representative method of the constraint-based approach is the PC algorithm (named after the first names its authors, Peter Spirtes and Clark Glymour) (Spirtes et al., 2000). Starting with a complete undirected graph where any two vertices are connected with each other, the PC algorithm first thins the complete graph by removing edges between vertices that are marginally independent. Then it removes edges by assessing conditional independence given one vertex, two vertices, and so on. Kalisch and Bühlmann (2007) proved the uniform consistency of the PC-algorithm in high-dimensional settings where $p = O(n^a)$ for $a > 0$. The results of the PC algorithm depend on the order of the edges to be assessed. Colombo and Maathuis (2012) proposed a modification of the PC algorithm that overcomes such order dependency.

This new method, named as PC-stable algorithm, can substantially improve the performance of the PC algorithm. We consider the PC-stable algorithm as the state-of-the-art method for high dimensional problems, and we will compare our method with the PC-stable algorithm.

The Independence Graph (IG) algorithm (Chapter 5.4.3 of Spirtes et al. (2000)) modifies the PC algorithm by using a different initial graph. Instead of starting with a complete undirected graph as the PC algorithm, the IG algorithm starts from an undirected independence graph, where two vertices are connected if the corresponding two variables are conditionally dependent given all the other variables. In such an independence graph (with the assumption of no estimation error), the neighbors of a vertex Y_j include its parents, children and co-parents in the underlying DAG, which constitute the so-called Markov blanket of Y_j such that Y_j is independent of all the other vertices given its Markov blanket (Aliferis et al., 2010). Under multivariate normal distribution assumption, independence graph is a Gaussian Graphic Model (GGM), and thus can be determined by the concentration matrix.

The Max-Min Hill-Climbing (MMHC) algorithm is a popular hybrid method that combines search-and-score approach and constraint-based approach (Tsamardinos et al., 2006). The MMHC first estimates the skeleton of the DAG using a constraint-based method (the Max-Min part of the algorithm), and then orient the edges using a search-and-score technique (the Hill-Climbing part of the algorithm). Schmidt et al. (2007) proposed to replace the Max-Min part of the MMHC algorithm by a penalized regression with L_1 penalty, which identifies the Markov blanket of each vertex and improves the performance of the MMHC algorithm. Meinshausen and Bühlmann (2006) studied the theoretical property of Markov blanket selection

using the Lasso (L_1) penalty, and they referred to this procedure as neighborhood selection. They pointed out that selection consistency of a variable Y 's Markov blanket, denoted by MB_Y , requires a so-called irrepresentable condition (Zhao and Yu, 2006) that there is weak correlation between the variables within and outside MB_Y . This is a strong condition and it generally does not hold for the genomic problems that motivate this study.

We propose a **PenPC** algorithm for DAG skeleton estimation in two steps. It first adapts neighborhood selection method to select Markov blanket of each vertex, and then it applies a modified PC-stable algorithm to remove false positive edges due to co-parents. Although the two-step approach of the **PenPC** algorithm shares similar spirit to the IG algorithm (Spirtes et al., 2000) and the modified MMHC algorithm (Schmidt et al., 2007), we have made the following novel contributions. First, we employ the log penalty $p(|b|; \lambda, \tau) = \lambda \log(|b| + \tau)$, one of the folded concave penalties (Fan and Lv, 2011), for the neighborhood selection step, which significantly improves the accuracy of Markov blanket search and allows much stronger correlation between the variables within and outside a Markov blanket than what is allowed for the Lasso penalty. Combining the neighborhood selection with log penalty and a novel modified PC-stable algorithm, the resulting **PenPC** algorithm outperforms the state-of-the-art PC-stable algorithm in terms skeleton estimation accuracy. In high dimensional setting, the **PenPC** algorithm also enjoys some advantage in terms of computational efficiency. Second, we provide theoretical justifications of the estimation consistency of the **PenPC** algorithm in high dimensional settings where $p = O(\exp\{n^a\})$ for $0 \leq a < 1$. We also discuss the implications for estimation consistency for two types of graphs: traditional random graph model where all the vertexes have the same

expected number of connections, and scale-free graph where a few vertices can have much larger number of neighbors than the other vertices. Whereas random graph is often assumed in previous studies, e.g., for the consistency of the PC algorithm (Kalisch and Bühlmann, 2007), scale-free graph is more frequently observed in gene networks as well as many other applications (Barabási and Albert, 1999).

3 Methods

We adopt a multivariate normal distribution assumption: $\mathbf{X} = (X_1, \dots, X_p)^T \sim N(0, \Sigma)$. Let $\mathbf{X} = (\mathbf{x}_1, \dots, \mathbf{x}_p)$ be the $n \times p$ observed data matrix. Without loss of generality, we assume each column \mathbf{x}_i ($1 \leq i \leq p$) has been standardized to have mean 0 and $\mathbf{x}_j^T \mathbf{x}_j = n$. Our PenPC algorithm proceeds in two steps: (1) neighborhood selection, and (2) application of a modified PC-stable algorithm to remove false connections.

Step 1. (Neighborhood Selection) We first select the neighborhood of vertex i by a penalized regression with X_i as response variable and all the other variables corresponding to vertices $V \setminus \{i\}$ as covariates:

$$\hat{\mathbf{b}}_i = \arg \min_{\mathbf{b}_i \in \mathbb{R}^{p-1}} \frac{1}{2} (\mathbf{x}_i - \mathbf{X}_{-i} \mathbf{b}_i)^T (\mathbf{x}_i - \mathbf{X}_{-i} \mathbf{b}_i) + n \sum_{j \neq i} p(|b_{i,j}|; \lambda_i, \tau_i). \quad (3)$$

where \mathbf{X}_{-i} is an $n \times (p-1)$ matrix for n measurements of the remaining $p-1$ covariates, $\mathbf{b}_i = (b_{i,1}, \dots, b_{i,i-1}, b_{i,i+1}, \dots, b_{i,p})^T$ and $p(|b_{i,j}|; \lambda_i, \tau_i)$ denotes a penalty function with tuning parameters λ_i and τ_i . We consider a class of folded concave penalty functions satisfying the following condition:

Condition 1: The penalty function $p(t; \lambda, \tau)$ is of the form $\lambda \rho(t; \tau)$, where

$\rho(t; \tau)$ is increasing and concave in $t \in [0, \infty)$ given τ and has continuous derivative $\rho'(t; \tau)$ in terms of t and with $\rho'(0+; \tau) > 0$.

This is a generalization of the Condition 1 in Fan and Lv (2011). Specifically, we employ the log penalty $p(|b|; \lambda, \tau) = \lambda \log(|b| + \tau)$, which has been demonstrated to have good performance in high-dimensional genetic studies (Sun et al., 2010). We employed the implementation of penalized regression with log penalty using coordinate descent algorithm (Sun et al., 2010), and the two tuning parameters λ and τ are selected by two-grid search to minimize extended BIC (Chen and Chen, 2008). After p penalized regressions for each of the p variables, we construct the GGM by adding an edge between vertices i and j if $\hat{b}_{ij} \neq 0$ or $\hat{b}_{ji} \neq 0$.

Step 2. (Modified PC-stable algorithm) We apply a modified PC-stable algorithm to remove the false edges due to co-parent relationships. For each edge $i - j$, we first assess marginal association between vertices i and j . If they remain dependent, we use the following strategy to search for candidate separation sets. Let

- $\mathbf{A}_{i,j} = [\text{adj}(i, \mathcal{C}_{\mathcal{G}}) \cup \text{adj}(j, \mathcal{C}_{\mathcal{G}})] \setminus \{i, j\}$, i.e., the union of the neighbors of i and j , except i or j themselves. \mathbf{A} is the Markov blanket of i and j .
- $\mathbf{B}_{i,j} = [\text{adj}(i, \mathcal{C}_{\mathcal{G}}) \cap \text{adj}(j, \mathcal{C}_{\mathcal{G}})] \setminus \{i, j\}$, i.e., the intersection of the neighbors of i and j , except i or j themselves.
- $\mathbf{C}_{i,j} = \{k : k \in \mathbf{A} \cap (\mathbf{B}_{i,j} \cup \text{Con}_{\mathcal{C}_{\mathcal{G}}}^{(i,j)}(\mathbf{B}_{i,j}))\}$, where $\text{Con}_{\mathcal{C}_{\mathcal{G}}}^{(i,j)}(\mathbf{B}_{i,j})$ is the set of vertices connected to any vertex in $\mathbf{B}_{i,j}$ by a chain of any length from a subgraph of $\mathcal{C}_{\mathcal{G}}$, which is created by removing vertices i and j as well as any edges connected to i or j . Obviously $\mathbf{B}_{i,j} \subseteq \mathbf{C}_{i,j}$.

Then the candidate conditional sets are

$$\mathbf{\Pi}_{i,j} = \{\mathbf{A} \setminus \mathbf{D}, \mathbf{D} \subseteq \mathbf{C}\}. \quad (4)$$

Note that in the definition of $\mathbf{\Pi}_{i,j}$, we skip the subscript i,j for \mathbf{A} , \mathbf{B} , \mathbf{C} , and \mathbf{D} to simplify notations. Each element of $\mathbf{\Pi}_{i,j}$ is a set $\mathbf{A} \setminus \mathbf{D}$, where \mathbf{D} is exhaustively searched across all subsets of \mathbf{C} . The number of candidate conditional sets are $2^{|\mathbf{C}|}$, which is often much smaller than all the conditional sets $2^{|\mathbf{A}|}$. More details are described in the Supplementary Materials, Section 2. An intuitive explanation is as follows. By Markov property in (2), the d-separation set of i and j consists of their parents, but not their shared children or descendants. All the parents of i or j belong to set \mathbf{A} . All the shared descents of i and j (among those within the the Markov blanket of i and j) belong to \mathbf{C} . Therefore we define $\mathbf{\Pi}_{i,j}$ such that it iteratively excludes any set of vertices that are likely to be the shared children/descendants of i and j .

We test the conditional independence of X_i and X_j given $\mathcal{K} \in \mathbf{\Pi}_{i,j}$ using Fisher transformation of partial correlation. Specifically, denote the partial correlation between X_i and X_j given $\mathcal{K} \in \mathbf{\Pi}_{i,j}$ by $\rho_{i,j|\mathcal{K}}$. With the significance level α , we reject the null hypothesis $H_0 : \rho_{i,j|\mathcal{K}} = 0$ against the alternative hypothesis $H_a : \rho_{i,j|\mathcal{K}} \neq 0$ if $\sqrt{n - |\mathcal{K}| - 3} \hat{z}_{i,j|\mathcal{K}} > \Phi^{-1}(1 - \alpha/2)$, where $\hat{z}_{i,j|\mathcal{K}} = 0.5 \log((1 + \hat{\rho}_{i,j|\mathcal{K}})/(1 - \hat{\rho}_{i,j|\mathcal{K}}))$ and $\Phi(\cdot)$ is the cdf of $N(0, 1)$.

The final output of **PenPC** algorithm is the estimated skeleton and separation sets $S(i, j)$ for all (i, j) . The separate sets are needed for causal effect estimation. If vertices i and j are not connected in the GGM (then they won't be connected in the skeleton), their separation set is all the remaining variables. If i and j are connected in both the GGM and the skeleton, there is no separation set. If i and j are connected

in the GGM, but not the skeleton, the separation set $S(i, j)$ is a set belongs to $\Pi_{i,j}$, such that the test $X_i \perp X_j \mid S(i, j)$ gives affirmative conclusion. Given the skeleton and the separation sets, causal effects can be assessed using function `idaFast` of R package `pcalg` (Kalisch et al., 2012).

4 Theoretical Properties

4.1 Fixed Graphs

We denote the L_2 and L_∞ norm of a matrix/vector by $\|\cdot\|_2$ and $\|\cdot\|_\infty$, respectively. The L_2 norm of a symmetric matrix is the maximum eigenvalue of the matrix. The L_∞ norm of a matrix is the maximum of the L_1 norm of each row. The L_∞ norm of a vector is the maximum of the absolute values of its elements. In this section we study high dimensional behavior where p grows as a function of sample size n . Thus we denote p as p_n , and denote a DAG and the corresponding GGM by $\mathcal{G}_n = (V_n, E_n)$ and $\mathcal{C}_{\mathcal{G}_n} = (V_n, F_n)$, respectively. We further denote the skeleton of \mathcal{G}_n by $\mathcal{G}_n^u = (V_n, E_n^u)$ where $a-b \in E_n^u \Leftrightarrow a \rightarrow b \in E_n$ or $b \rightarrow a \in E_n$. For any vertex i , denote the observed data of the variables within and outside of $\text{adj}(i, \mathcal{C}_{\mathcal{G}_n})$ (but not including \mathbf{x}_i) by \mathcal{X}_{i1} and \mathcal{X}_{i2} , respectively. If the penalty function has continuous second derivative, we define $\kappa(\mathbf{v}; \lambda, \tau) = \max_{1 \leq j \leq r} -\lambda \rho''(|v_j|; \tau)$, where for $\mathbf{v} = (v_1, \dots, v_r)^T \in \mathbb{R}^r$ and $v_j \neq 0$; otherwise we replace $\rho''(|v_j|; \tau)$ by $\lim_{\epsilon \rightarrow 0+} \sup_{t_1 < t_2 \in (|v_j|-\epsilon, |v_j|+\epsilon)} \frac{\rho'(t_2; \tau_i) - \rho'(t_1; \tau_i)}{t_2 - t_1}$.

The following conditions are needed for the consistency of the **PenPC** algorithm.

(A1) Dimensionality of the problem. $p_n = O(\exp\{n^a\})$ with $a \in [0, 1)$.

(A2) Sparseness assumption. Let $q_n = \max_{1 \leq j \leq p_n} |\text{adj}(j, \mathcal{C}_{\mathcal{G}_n})|$, i.e., the maximum

degree of $\mathcal{C}_{\mathcal{G}_n}$. $q_n \leq O(n^b)$ for some $0 \leq b < 1$. By the following Lemma 2, $\max_{1 \leq j \leq p_n} |\text{adj}(j, \mathcal{G}_n)| \leq q_n$.

(A3) Minimum effect size for neighborhood selection. $\delta_n \equiv (1/2) \inf_{i,j} \{|b_{i,j}| : b_{i,j} \neq 0\} \geq$

$O(n^{-d_2})$ with $0 < d_2 < (1-a)/2 - s_0$, where s_0 is a constant describing the correlation structure of the covariates with non-zero effect: $\|(\mathcal{X}_{i1}^T \mathcal{X}_{i1})^{-1}\|_\infty = O(n^{-1+s_0})$ with $0 \leq s_0 < (1-a)/2$.

(A4) Conditions for penalty function. $p'(\delta_n; \lambda_i, \tau_i) \ll n^{-d_2-s_0}$, $p'(0+; \lambda_i, \tau_i) \gg n^{-1/2+a/2+b} \sqrt{\log n}$.

(A5) Further conditions for penalty function with respect to covariance structure of

the covariates. For all $i = 1, \dots, p$ and $0 < K < 1$, $\|\mathcal{X}_{i2}^T \mathcal{X}_{i1} (\mathcal{X}_{i1}^T \mathcal{X}_{i1})^{-1}\|_\infty \leq \min(K \frac{\rho'(0+; \tau_i)}{\rho'(\delta_n; \tau_i)}, O(n^b))$ and $\|(\mathcal{X}_{i1}^T \mathcal{X}_{i1})^{-1}\|_2 < 1/(n\kappa_0)$, where $\kappa_0 = \max_{\beta_1 \in \mathcal{N}_{i1}} \kappa(\beta_1; \lambda_i, \tau_i)$, and \mathcal{N}_{i1} is a hypercube around \mathbf{b}_{i1} (a sub-vector of \mathbf{b}_i 's non-zero components) such that $\|\beta_1 - \mathbf{b}_{i1}\|_\infty \leq Cn^{-d_2}$.

(A6) Restriction on the size of conditional partial correlation. Denote the partial correlations between X_i and X_j given a set of variables $\{X_r : r \in \mathcal{K}\}$ for $\mathcal{K} \subseteq V_n \setminus \{i, j\}$ by $\varrho_{i,j|\mathcal{K}}$. For $\mathcal{K} \in \Pi_{ij}$, the absolute values of $\varrho_{i,j|\mathcal{K}}$'s are bounded:

$$\inf_{i,j,\mathcal{K}} \{|\varrho_{i,j|\mathcal{K}}| : \rho_{i,j|\mathcal{K}} \neq 0, \mathcal{K} \in \Pi_{ij}\} \geq c_n, \text{ and } \sup_{i,j,\mathcal{K}} \{|\varrho_{i,j|\mathcal{K}}| : \mathcal{K} \in \Pi_{ij}\} \leq M < 1,$$

where $c_n = O(n^{-d_1})$ for some $0 < d_1 < \min\{(1-a)/2, (1-b)/2\}$.

The sparseness assumption (A2) will be replaced by tighter assumptions for two specific random graph models later. Assumptions (A3)-(A5) ensure that the step 1 of **PenPC** can recover the GGM. Assumption (A6) ensures the summation of the

mistaken probabilities of the step 2 of the PenPC algorithm goes to 0 asymptotically. The condition $\|\mathcal{X}_{i2}^T \mathcal{X}_{i1} (\mathcal{X}_{i1}^T \mathcal{X}_{i1})^{-1}\|_\infty \leq K \rho'(0+; \tau_i) / \rho'(\delta_n; \tau_i)$ in Assumption (A5) deserves more discussion since it reveals why our neighborhood selection method using log penalty can perform better than the Lasso. For the Lasso, there is no extra parameter τ_i and $\rho(t) = |t|$, and thus $\rho'(0+)/\rho'(\delta_n) = 1$. Therefore the condition becomes $\|\mathcal{X}_{i2}^T \mathcal{X}_{i1} (\mathcal{X}_{i1}^T \mathcal{X}_{i1})^{-1}\| \leq K$, which is equivalent to the irrerepresentable condition. In contrast, for the log penalty, $\rho'(t; \tau_i) = \text{sgn}(t)/(|t| + \tau_i)$, and thus $\rho'(0+; \tau_i) / \rho'(\delta_n; \tau_i) \rightarrow (\delta_n + \tau_i) / \tau_i$, which can go to infinity if $\tau_i = o(\delta_n)$. More specifically, the scale of $\rho'(0+; \tau_i) / \rho'(\delta_n; \tau_i)$ can be derived as follows. By assumption A4, $\rho'(0+; \tau_i) / \rho'(\delta_n; \tau_i) \gg (n^{-1/2+a/2+b} \sqrt{\log n}) / (n^{-d_2-s_0}) = n^b \sqrt{\log n} \rightarrow \infty$, where the last equality is due to Assumption A3. We can show that the log penalty satisfies other assumptions and refer the readers to Chen et al. (2014) for details.

The following Lemma 1 claims that the support of the regression coefficients is the same as that of the concentration matrix. Therefore, we can use the regression model to estimate the GGM $\mathcal{C}_{\mathcal{G}_n}$.

Lemma 1. *Suppose $X = (X_1, \dots, X_p)^T \sim \mathcal{N}_p(\boldsymbol{\mu}, \boldsymbol{\Sigma})$ and $\boldsymbol{\Omega} = \boldsymbol{\Sigma}^{-1}$. Then*

$$X_i = X_{-i}^T \mathbf{b}_i + \epsilon_i, \quad (5)$$

where X_{-i} denotes a random vector derived from X by removing X_i from X , $\mathbf{b}_i = -\sigma_i^2 \boldsymbol{\Omega}_{-i,i}$, and $\epsilon_i \sim \mathcal{N}(0, \sigma_i^2)$, with $\sigma_i^2 = \Sigma_{ii} - \Sigma_{i,-i} (\Sigma_{-i,-i})^{-1} \Sigma_{-i,i}$. Σ_{ab} and $\boldsymbol{\Omega}_{ab}$ are the sub-matrices where the subscripts a and b indicate inclusion/exclusion of certain random variables.

The proof of Lemma 1 is omitted since it is straightforward conclusion based on conditional distribution of multivariate normal random variables.

Consider the neighborhood selection problem for one of the variables versus all the other variables. Let $\mathcal{S}_i = \text{supp}(\mathbf{b}_i)$ be the support of the true regression coefficient \mathbf{b}_i with size $|\mathcal{S}_i| = s_i$. From Lemma 1, the degree of vertex i in $\mathcal{C}_{\mathcal{G}_n}$ is s_i . Recall that in assumption (A4) \mathcal{X}_{i1} and \mathcal{X}_{i2} denote the observed data of the variables corresponding to $\mathcal{S}_i \subseteq V_n \setminus \{i\}$ and its complement, $\mathcal{S}_i^c = V_n \setminus (\mathcal{S}_i \cup \{i\})$. Similarly \mathbf{b}_{i1} and $\hat{\mathbf{b}}_{i1}$ are respectively the sub-vectors of \mathbf{b}_i and $\hat{\mathbf{b}}_i$ corresponding to \mathcal{S}_i .

Theorem 1. *Given Assumptions (A1) - (A5), with probability at least $1 - C \exp\{n^a - n^a \log(n)\}$ for a constant $0 < C < \infty$, there exists a local minimizer $\hat{\mathbf{b}}_i = (\hat{\mathbf{b}}_{i1}, \hat{\mathbf{b}}_{i2})^T$ that satisfies the following conditions: for any $i = 1, \dots, p_n$,*

(a) *Sparsity: $\hat{\mathbf{b}}_{i2} = \mathbf{0}$.*

(b) *L_∞ loss: $\|\hat{\mathbf{b}}_{i1} - \mathbf{b}_{i1}\|_\infty = o(n^{-d_2})$, where d_2 is defined in (A3).*

The proof is in the Supplementary Materials. Under assumption (A1), the dimensionality p_n is allowed to grow up to exponentially fast with sample size n . The value of d_2 can be as large as $1/2$ depending on the lower bound of effect size specified in assumption (A3).

Corollary 1 is a simple extension from Theorem 1. It characterizes the consistency of the p_n penalized regression models which estimate the GGM $\mathcal{C}_{\mathcal{G}_n}$. Denote $\hat{\mathcal{C}}_{\mathcal{G}_n}(\boldsymbol{\theta})$ as the estimate of $\mathcal{C}_{\mathcal{G}_n}$ by the neighborhood selection, where $\boldsymbol{\theta}$ are tuning parameters of the penalty function.

Corollary 1. *Given Assumption (A1), (A4)-(A6),*

$$\mathbb{P}(\hat{\mathcal{C}}_{\mathcal{G}_n}(\boldsymbol{\theta}) = \mathcal{C}_{\mathcal{G}_n}) \geq 1 - C \exp\{2n^a - n^a \log(n)\}$$

for a constant $0 < C < \infty$.

Lemma 2. *If the distribution P_X is Markov to \mathcal{G} , i.e., if the joint density f_X satisfies the recursive factorization, the set of edges F_n of $\mathcal{C}_{\mathcal{G}_n}$ includes all edges E_n^u of \mathcal{G}_n^u plus co-parent relationship in \mathcal{G}_n .*

This lemma 2 has been proved in Lemma 3.21 of Lauritzen (1996).

Lemma 3. *Assume (A1). If $(i, j) \in F_n$ of $\mathcal{C}_{\mathcal{G}_n}$ but $(i, j) \notin E_n^u$ of \mathcal{G}_n^u , the conditioning set $\Pi_{i,j}$ in (4) includes at least one set which d-separates vertices i and j in \mathcal{G} .*

The proof of Lemma 3 is presented in the Supplementary Materials. Lemma 2 and Lemma 3 provide the theoretical justifications for using GGM as a starting point of our modified PC-algorithm. Lemma 2 shows that if we have a perfect estimation of the concentration matrix, we can recover all the edges in the skeleton with no false negatives, but some false positives: the co-parent relationships. Lemma 3 presents that we can remove the false positives due to co-parent relationship by examining partial correlation conditioning on some set in $\Pi_{i,j}$.

Next we discuss the theoretical property of the modified PC-stable algorithm (the second step of the **PenPC** algorithm) given a perfect estimation of GGM. Later we will show that the summation of mistaken probabilities of GGM estimation and skeleton estimation given GGM goes to 0 as $n \rightarrow \infty$.

Theorem 2. *Let α_n be the p -value threshold for testing whether a partial correlation is 0. Let $\hat{\mathcal{G}}_n^u(\alpha_n)$ be the estimates of \mathcal{G}_n^u from the second step of the **PenPC** algorithm given a perfect estimation of GGM from the first step of the **PenPC** algorithm. Assume (A1), (A2) and (A6), then there exists $\alpha_n \rightarrow 0$, such that*

$$\mathbb{P} \left[\hat{\mathcal{G}}_n^u(\alpha_n) = \mathcal{G}_n^u \right] = 1 - O \left(\exp \{ -Cn^{1-2d_1} \} \right) \rightarrow 1,$$

where $0 < C < \infty$ is a constant.

The proof is in the Supplementary Materials. Similar theorem has been proved in Kalisch and Bühlmann (2007) with p_n at polynomial order of n . By exploiting accurate estimation of GGM, we extend the theorem to $p_n = O(\exp\{n^a\})$ case. Corollary 2 provides the combined error of step 1 and step 2 of **PenPC** algorithm as a simple extension of Corollary 1 and Theorem 2.

Corollary 2. *Let $\hat{\mathcal{G}}_n^u(\boldsymbol{\theta}, \alpha_n)$ be the estimates of \mathcal{G}_n^u from the two-step approach **PenPC** algorithm. Assume (A1)-(A6), then there exists an $\alpha_n \rightarrow 0$, such that*

$$\mathbb{P} \left[\hat{\mathcal{G}}_n^u(\boldsymbol{\theta}, \alpha_n) = \mathcal{G}_n^u \right] = 1 - O \left(\exp\{-Cn^{1-2d_1}\} \right) \rightarrow 1,$$

where $0 < C < \infty$ is a constant.

4.2 Random Graphs

Under certain conditions, the theoretical results could also be extended to two commonly used models for random graphs: Erdős and Rényi (ER) Model (Erdős and Rényi, 1960) and Barabási and Albert (BA) Model (Barabási and Albert, 1999). In general, assumption (A2) no longer holds for random graphs. However, based on the proof in the Supplementary Materials, it is easy to see that assumption (A2) can be relaxed to (A2').

(A2') Let $q_n = \max_{1 \leq j \leq p_n} |\text{adj}(j, \mathcal{C}_{\mathcal{G}_n})|$. Assume

$$\mathbb{P}\{q_n \leq O(n^b)\} = 1, \quad \text{for some } 0 \leq b < 1.$$

It is then suffices to show assumption (A2') holds. Note that the value of b in this assumption will affect the minimum effect size of partial correlations in assumption (A3) and the convergence probability in Theorem 1 and Corollary 1.

4.2.1 Erdős and Rényi (ER) Model

The ER model constructs a graph $G(p_n, p_E)$ of p_n vertices by connecting vertices randomly. Each edge is included in the graph with probability p_E independent from all other edges. By law of large numbers, such vertex is almost surely connected to $(p_n - 1)p_E$ edges. Let M_n be the maximal degree of the graph. Erdős and Rényi (1960) proved the following results about M_n .

Lemma 4. *In the graph $G(p_n, p_E)$ following the ER model, the maximal degree M_n almost surely converges to m_n , where*

$$m_n = \begin{cases} O(\log p_n), & \text{if } p_n p_E < 1, \\ p_n^{2/3}, & \text{if } p_n p_E = 1, \\ O(p_n), & \text{if } \lim_{p_n \rightarrow \infty} p_n p_E = c > 1. \end{cases}$$

When $p_n = O\{\exp(n^a)\}$, by Lemma 4, assumption (A2') holds immediately if $p_n p_E < 1$ and $b \geq a$. When $p_n p_E \geq 1$, our proof cannot handle the general case $p_n = O\{\exp(n^a)\}$. However, when the number of vertices is of the polynomial order of n , assumption (A2') may still hold. In particular, suppose $p_n = O(n^r)$. When $p_n p_E < 1$, assumption (A2') holds for any $b \in [0, \infty)$. When $p_n p_E = 1$, assumption (A2') holds if $b \geq 2r/3$. When $p_n p_E \rightarrow c > 1$, assumption (A2') holds if $r < 1$ and $b \geq r$.

4.2.2 Barabási and Albert (BA) Model

The BA model is used to generate scale free graphs whose degree distribution follows a power law: $\mathbb{P}(\nu) = \gamma_0 \nu^{-\gamma_1}$, with a normalizing constant γ_0 and a exponent γ_1 . Specifically, BA model generates a graph by adding vertices into the graph over time

and when each new vertex is introduced into the graph, it is connected with larger probability to the existing vertices with larger number of connections. Since the distribution does not depend on the size of the network (or time), the graph organizes itself into a scale free state (Barabási and Albert, 1999). Móri (2005) showed that M_n (the maximal degree of the graph) almost surely converges to $O(p^{1/2})$. Thus, assumption (A2') holds for the case $p_n = O(n^r)$ with $b \leq r/2$.

5 Simulation Studies

We evaluated the performance of the **PenPC** algorithm and the PC-stable algorithm in terms of sensitivity and specificity of skeleton estimation using DAGs simulated by the ER model or the BA model. In both simulations and real data analysis, we used the implantation of the PC-stable algorithm by function `skeleton` in R package `pcalg` (version 1.1-6), and we have implemented **PenPC** algorithm in R package **PenPC**.

Following Kalisch and Bühlmann (2007), we simulated DAGs of p vertices by the ER model as follows. First we assumed the p vertices were ordered so that if $i < j$, vertex i could only be the parent rather than child of vertex j . Then for any vertex pair (i, j) where $i < j$, we added an edge $i \rightarrow j$ with probability p_E . For the BA model, the DAGs were simulated following Barabási and Albert (1999). The initial graph had one vertex and no edge. Then a new vertex was added in each step and directed edges were added so that they started from the new vertex and pointed to some of the existing vertices. Specifically, in the $(t + 1)$ -th step, e edges were proposed. For each edge, the new vertex was connected to the i -th ($1 \leq i \leq t$) existing vertex with probability $\nu_i^{(t)} / \sum_j \nu_j^{(t)}$, where $\nu_i^{(t)} = |\text{adj}(i, \mathcal{G}^{(t)})|$, and $\mathcal{G}^{(t)}$ was

the DAG at the t -th step, right before adding the new vertex. Figure 2 shows the distribution of the degrees ν from simulated DAGs under ER model ($p = 1000$ and $p_E = 2/p$) and BA model ($p = 1000$ and $e = 1$). The probability of finding a highly

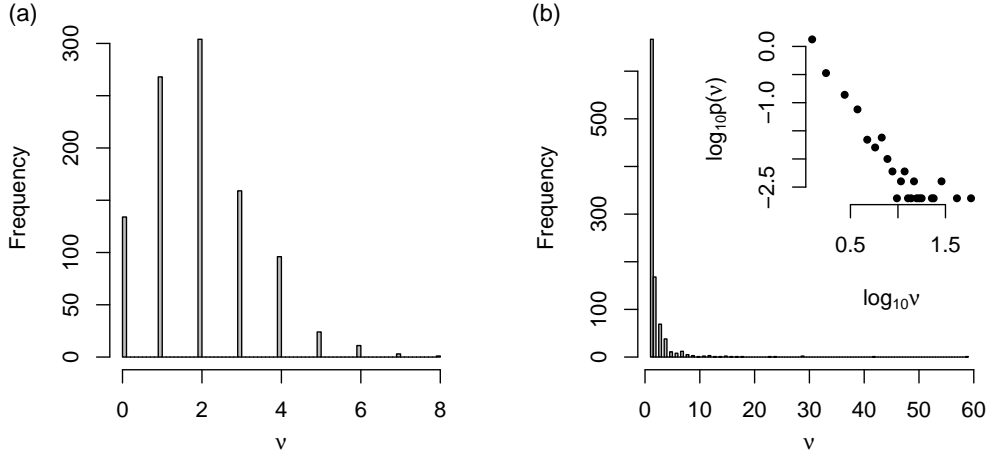


Figure 2: Histograms of the degree ν . (a) ER model with $p = 1000$ and $p_E = 2/p$. (b) BA model with $p = 1000$ and $e = 1$ and the \log_{10} scale density of $\log_{10} \nu$ in its subplot.

connected vertex decreases exponentially with ν for the graphs generated by the ER model (Figure 2(a)). However, for the graphs generated by the BA model, highly connected vertices with large ν have relatively large chance of occurring (Figure 2(b)), and there is a linear relation between degree and degree probability in log-log scale, which confirms the scale-free property of the graphs generated by the BA model. Similar conclusions apply for the graphs generated by the BA model with $e = 2$ (Figure S1 of the Supplementary Materials).

After constructing the DAGs, the observed were are simulated by structure equa-

tions under multivariate normal assumption. For example, denote the parents of X_j by pa_j , then $\mathbf{x}_j = \sum_{k \in \text{pa}_j} b_{jk} \mathbf{x}_k + \epsilon_j$, where $\epsilon_j \sim \mathcal{N}(0, \sigma^2 I_{n \times n})$. In our simulations, all b_{jk} 's and σ^2 were set to be 1. Our simulation settings were displayed in Table 1. For

Table 1: Simulation Setting			
p	n	p_E (ER)	e (BA)
11	100	0.2	1,2
100	30	0.02, 0.03, 0.04, 0.05	1,2
1000	300	0.002, 0.005, 0.01	1,2

either ER or BA model, we considered low dimension setting where $p = 11, n = 100$ and high-dimension settings where $p = 100, n = 30$ and $p = 1000, n = 300$ with various sparsity levels determined by P_E for ER model and e for BA model. Due to limited space, here we only show the results for the simulation setups using ER model ($p = 1000, n = 300, p_E = 0.005$) or BA model ($p = 1000, n = 300, e = 1$), and other results are presented in Figure S3 - Figure S15 of the Supplementary Materials.

There are three tuning parameters. λ and τ are tuning parameters for the penalty function of the **PenPC** algorithm. α is the p-value cutoff used by the PC-stable algorithm or our modified PC-stable algorithm to declare conditional independence. We chose λ and τ by extended BIC (Chen and Chen, 2008), and examined the results of PC or **PenPC** across various values of α . In the upper panels of Figure 3, we showed the performances of three methods: PC (PC-stable algorithm), Pen (penalized regression only, step 1 of the **PenPC**), and **PenPC** when $\alpha = 0.01$ and the skeleton was simulated by the ER model. The penalized regression identifies

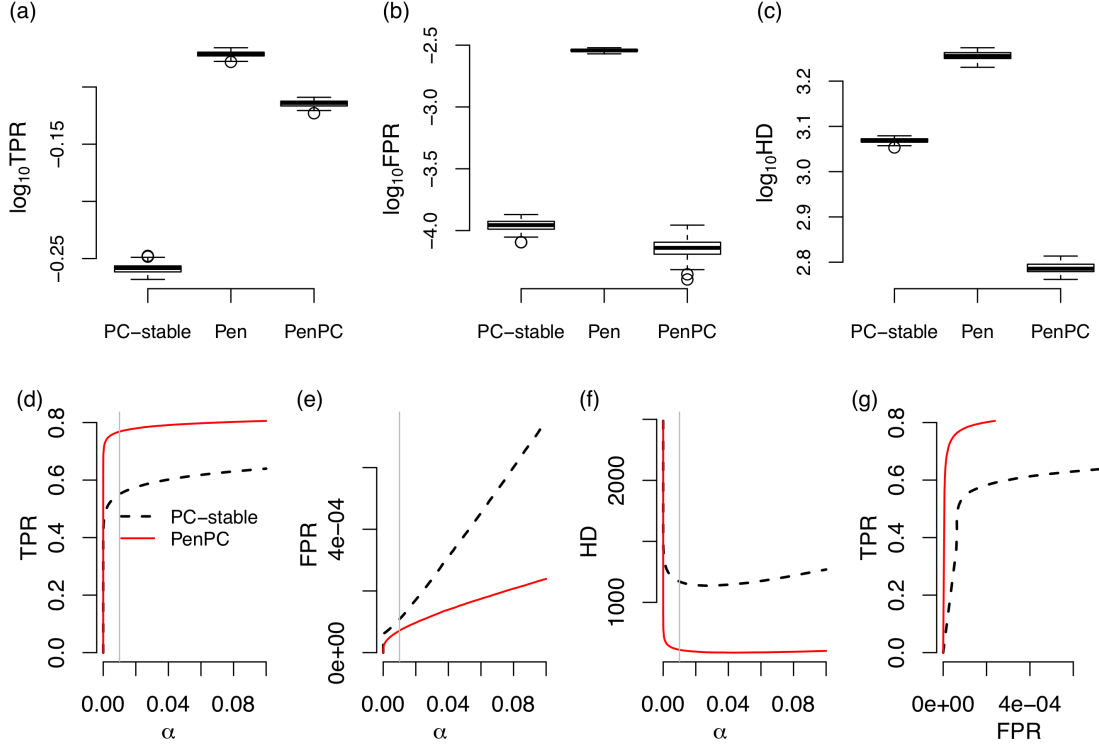


Figure 3: Performance of ER model ($p = 1000, n = 300, p_E = 0.005$). The upper panels are box plots (in \log_{10} scale) of true positive rate (TPR) (a), false positive rate (FPR) (b) and hamming distance (HD) (c) from 100 replications at $\alpha = 0.01$. The lower panels are average true positive rate (d), false positive rate (e), and Hamming distance (f) from 100 replications when the tuning parameter α is changed from 0 to 0.1 (the grey vertical line are at $\alpha = 0.01$). ROC curves are shown in panel (g).

more true positives than the PC-stable algorithm, but also introduce more false positives (Figure 3 (a-b)), while PenPC algorithm significantly reduces the number of false positives, though some true positives are also removed. At the end, the PenPC has the lowest number of false positives plus false negatives, as measured by

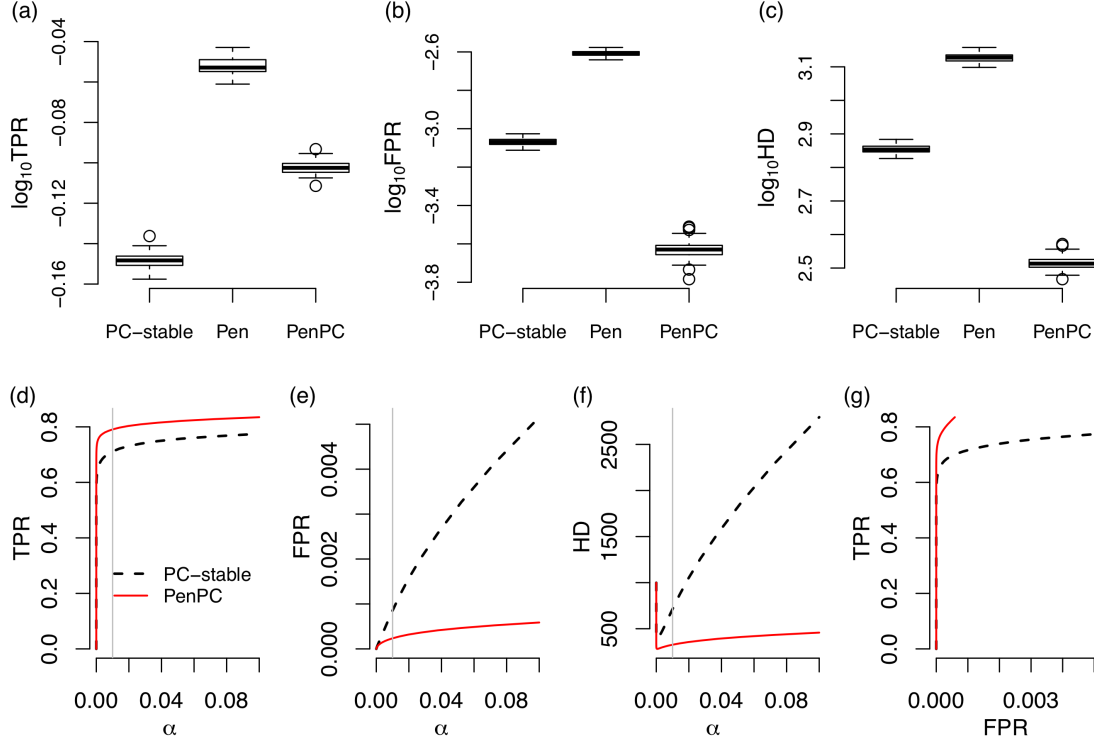


Figure 4: Performance of BA model (p=1000,n=300,e=1). The upper panels are box plots (in \log_{10} scale) of true positive rate (TPR) (a), false positive rate (FPR) (b) and hamming distance (HD) (c) from 100 replications at $\alpha = 0.01$. The lower panels are average true positive rate (d), false positive rate (e), and Hamming distance (f) from 100 replications when the tuning parameter α is changed from 0 to 0.1 (the grey vertical line are at $\alpha = 0.01$). ROC curves are shown in panel (g).

Hamming distance (HD) (Figure 3 (c)). Figures 3(d-f) show that across various cutoff values of α , PenPC consistently has better performance than the PC-stable algorithm. Finally, Figure 3(g) shows the ROC curves for the PenPC and the PC-stable algorithms, which illustrate that PenPC has better sensitivity and specificity

than the PC-stable algorithm regardless of the cutoff α . Similar conclusions can be drawn for the simulation results shown in Figure 4, where the DAGs are simulated by the BA model.

6 Application

We applied the PC algorithm and the PenPC algorithm to study gene-gene network using gene expression data from tumor tissue of breast cancer patients. Gene expression were measured by RNA-seq (Network et al., 2012). We quantified the expression of each gene within each sample by $\log(\text{total read count})$, or in short, logTReC. We restricted our study on 550 female caucasian samples. After removing genes with low expression across most samples, we ended up with 18,827 genes. In this analysis, we focused on 410 genes from the cancer Gene Census in <http://cancer.sanger.ac.uk/cancergenome/projects/census/>. We chose this relatively small gene set for two reasons. One is that it is easier to exploit the results given that these genes have better cancer-related annotations. The other reason is that we would like to compare the results of the PC algorithm and the PenPC algorithm. However, when we worked on a larger gene set of more than 8,000 genes, the PC algorithm took too much time to finish the computation. We defer the discussion of computational efficiency in the discussion section.

Several covariates may influence the correlations across genes. We removed such effects by taking residuals of logTReC data for each gene using a linear regression model with the following covariates: 75 percentile of logTReC per sample, which captures read depth, plate, institution, age, and 6 genotype PCs. Then

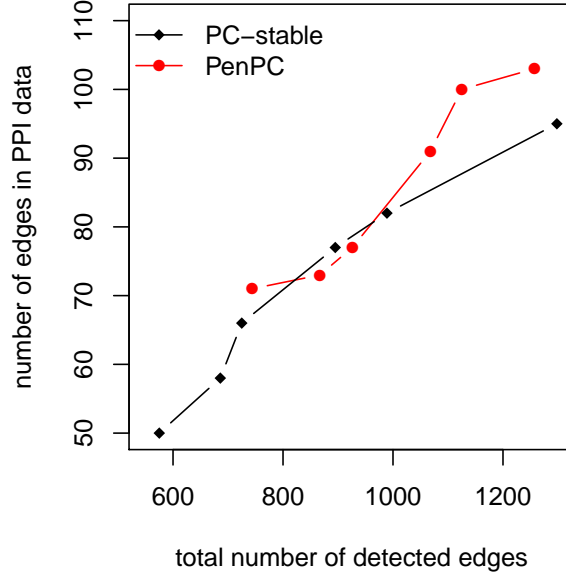


Figure 5: Comparing PenPC algorithm with PC-stable algorithm in terms of skeleton estimation by changing the significance levels for partial correlation testings, $\alpha = 0.0001, 0.0005, 0.001, 0.005, 0.01$ and 0.05 .

for $\alpha = 0.0001, 0.0005, 0.001, 0.005, 0.01$ and 0.05 , we estimated the skeleton by the PC-stable and PenPC algorithms. The estimated skeletons were evaluated by comparing the estimated edge sets with protein-protein interaction (PPI) database at <http://www.pathwaycommons.org/pc2/downloads.html>, and we used the protein annotations from the Universal Protein Resource (<http://www.uniprot.org>). There were 3315 PPIs where both proteins were matched to the 410 genes in our gene expression data. Figure 5 shows the total number of detected edges versus the number of edges in PPI data. For both methods, the total number of detected edges increase monotonically as α increases. The PenPC algorithm consistently detects more or comparable number of edges than PC-stable algorithm, which reflects the

sensitivity, given the same total number of edges, which reflects the specificity.

7 Conclusions

We propose a two-step approach, **PenPC** algorithm, to estimate the skeletons of high dimensional DAGs. We show that the **PenPC** algorithm provides asymptotically consistent estimate of the skeleton of a high dimensional DAG. For fixed graphs, the number of vertices p_n could be exponential scale of the sample size n . We also considered two commonly used random graph models and discussed in detail the conditions under which the consistency properties hold. The simulation studies and real data analysis show that the network skeletons estimated by **PenPC** can be substantially more accurate than those estimated by the PC-stable algorithm. Although **PenPC** performs well for the scale-free network, further improvement is possible by incorporating a regularization method which prefers to the scale-free structure (Liu and Ihler, 2011) in the first step of the **PenPC**.

The acyclic assumption may appear restrictive for gene-gene network since there may be feed back loops in gene expression regulation. One solution is to use structure equation models (SEMs) where loops are allowed (Li et al., 2006). Recently, a few methods have been developed to add penalization into the SEM (Logsdon and Mezey, 2010), and we conjecture that adopting folded concave penalties in these methods may further improve their performance. The other solution is to construct Dynamic Bayesian Network using time course data (Husmeier, 2003). This becomes a situation where the natural ordering of the variables are available through time information, and thus penalized regression itself is able to identify the DAG skeleton through

estimating conditional auto-regressive correlations. The main challenge would be that the time course data usually have limited number of time points and thus augmenting data from other sources would be useful.

The computational efficiency of the PC-stable algorithm and our modified PC-stable algorithm increases as the number of vertices increases and as the p-value cutoff increases. When the dimension of the problem becomes high enough, PC-stable algorithm becomes computationally inefficient. We discuss the computational efficiencies in two settings where $p = 410$ or $p = 8,261$. In our real data analysis where $n = 550$ and $p = 410$. On average the step 1 of the **PenPC** algorithm took 3 seconds for one penalized regression, including searching for the best tuning parameter combination across a $100(\lambda) \times 10(\tau)$ two-dimensional grid. Thus the total computational time is $3 \times 410/60 = 20.5$ minutes. As p-value cutoff varies from 10^{-4} to 0.05, the computational time of the PC algorithm increases from 3 minutes to 54 minutes, while the computational time of the 2nd step of the **PenPC** algorithm increases from 17 seconds to 8 minutes. Overall the computational time of the two methods are comparable and certainly **PenPC** is computationally more attractive if one wants to examine the results across multiple p-value cutoffs. We also examine the computational efficiency when we expand the number of genes to $p=8,261$. The step 1 in **PenPC** algorithm took 128 seconds for one penalized regression, including tuning parameter selection across a 100×10 two-dimensional grid. This step, although computationally expensive, can be easily paralleled. Given the GGM, the 2nd step of the **PenPC** is computationally much more efficient than the PC-stable algorithm (Figure 6). For example, with p-value threshold varies from 10^{-7} to 10^{-5} , the computational time of the PC algorithm increases from 20 hours to 50 hours, and

we did not run PC algorithm for p-value larger than 10^{-5} due to high computational burden. In contrast, the computation time of the **PenPC** remains below 10 hours even for p-value cutoff 5×10^{-3} . All the computation are done in Linux server with an 2.93 GHz Intel processor and 48GB RAM.

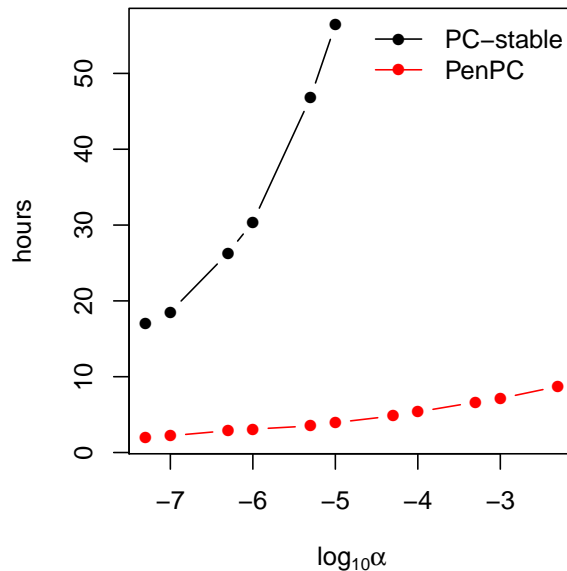


Figure 6: Computation time for PC-stable and step 2 of **PenPC**.

References

Aliferis, C. F., Statnikov, A., Tsamardinos, I., Mani, S., and Koutsoukos, X. D. (2010). Local causal and markov blanket induction for causal discovery and feature selection for classification part ii: Analysis and extensions. *The Journal of Machine Learning Research*, 11:235–284.

- Barabási, A. and Albert, R. (1999). Emergence of scaling in random networks. *science*, 286(5439):509–512.
- Chen, J. and Chen, Z. (2008). Extended bayesian information criteria for model selection with large model spaces. *Biometrika*, 95(3):759–771.
- Chen, T., Sun, W., and Fine, J. (2014). Designing penalty functions in high dimensional problems: The role of tuning parameters. Technical report, University of North Carolina, Chapel Hill.
- Chickering, D. M. (2003). Optimal structure identification with greedy search. *The Journal of Machine Learning Research*, 3:507–554.
- Colombo, D. and Maathuis, M. (2012). A modification of the pc algorithm yielding order-independent skeletons. *arXiv preprint arXiv:1211.3295*.
- Erdős, P. and Rényi, A. (1960). On the evolution of random graphs. *Publications of the Mathematical Institute of the Hungarian Academy of Sciences*, 5:17–61.
- Fan, J. and Lv, J. (2011). Nonconcave penalized likelihood with np-dimensionality. *Information Theory, IEEE Transactions on*, 57(8):5467–5484.
- Heckerman, D., Geiger, D., and Chickering, D. (1995). Learning bayesian networks: The combination of knowledge and statistical data. *Machine learning*, 20(3):197–243.
- Husmeier, D. (2003). Sensitivity and specificity of inferring genetic regulatory interactions from microarray experiments with dynamic bayesian networks. *Bioinformatics*, 19(17):2271–2282.

- Kalisch, M. and Bühlmann, P. (2007). Estimating high-dimensional directed acyclic graphs with the pc-algorithm. *The Journal of Machine Learning Research*, 8:613–636.
- Kalisch, M., Mächler, M., Colombo, D., Maathuis, M., and Bühlmann, P. (2012). Causal inference using graphical models with the r package pcalg. *Journal of Statistical Software*, 47(11):1–26.
- Lauritzen, S. (1996). *Graphical models*, volume 17. Oxford University Press, USA.
- Li, R., Tsaih, S.-W., Shockley, K., Stylianou, I. M., Wergedal, J., Paigen, B., and Churchill, G. A. (2006). Structural model analysis of multiple quantitative traits. *PLoS genetics*, 2(7):e114.
- Liu, Q. and Ihler, A. T. (2011). Learning scale free networks by reweighted l1 regularization. In *International Conference on Artificial Intelligence and Statistics*, pages 40–48.
- Logsdon, B. A. and Mezey, J. (2010). Gene expression network reconstruction by convex feature selection when incorporating genetic perturbations. *PLoS computational biology*, 6(12):e1001014.
- Maathuis, M., Colombo, D., Kalisch, M., and Bühlmann, P. (2010). Predicting causal effects in large-scale systems from observational data. *Nature Methods*, 7(4):247–248.
- Maathuis, M., Kalisch, M., and Bühlmann, P. (2009). Estimating high-dimensional intervention effects from observational data. *The Annals of Statistics*, 37(6A):3133–3164.

- McLendon, R., Friedman, A., Bigner, D., Van Meir, E. G., Brat, D. J., Mastrogiannis, G. M., Olson, J. J., Mikkelsen, T., Lehman, N., Aldape, K., et al. (2008). Comprehensive genomic characterization defines human glioblastoma genes and core pathways. *Nature*, 455(7216):1061–1068.
- Meek, C. (1995). Strong completeness and faithfulness in bayesian networks. In *Proceedings of the Eleventh conference on Uncertainty in artificial intelligence*, pages 411–418. Morgan Kaufmann Publishers Inc.
- Meinshausen, N. and Bühlmann, P. (2006). High-dimensional graphs and variable selection with the lasso. *The Annals of Statistics*, 34(3):1436–1462.
- Móri, T. (2005). The maximum degree of the barabási-albert random tree. *Combinatorics Probability and Computing*, 14(3):339–348.
- Network, C. G. A. et al. (2012). Comprehensive molecular portraits of human breast tumours. *Nature*, 490(7418):61–70.
- Pearl, J. (2009). *Causality: models, reasoning and inference*. Cambridge Univ Press.
- Schmidt, M., Niculescu-Mizil, A., and Murphy, K. (2007). Learning graphical model structure using l1-regularization paths. In *AAAI*, volume 7, pages 1278–1283.
- Shojaie, A. and Michailidis, G. (2010). Penalized likelihood methods for estimation of sparse high-dimensional directed acyclic graphs. *Biometrika*, 97(3):519–538.
- Spirtes, P., Glymour, C., and Scheines, R. (2000). *Causation, prediction and search*, volume 81. The MIT Press.

- Sun, W., Ibrahim, J. G., and Zou, F. (2010). Genomewide multiple-loci mapping in experimental crosses by iterative adaptive penalized regression. *Genetics*, 185(1):349–359.
- Teyssier, M. and Koller, D. (2005). Ordering-based search: A simple and effective algorithm for learning bayesian networks. In *In UAI*, pages 584–590.
- Tsamardinos, I., Brown, L. E., and Aliferis, C. F. (2006). The max-min hill-climbing bayesian network structure learning algorithm. *Machine learning*, 65(1):31–78.
- van de Geer, S. and Bühlmann, P. (2013). ℓ_0 -penalized maximum likelihood for sparse directed acyclic graphs. *The Annals of Statistics*, 41(2):536–567.
- Vogelstein, B., Papadopoulos, N., Velculescu, V. E., Zhou, S., Diaz, L. A., and Kinzler, K. W. (2013). Cancer genome landscapes. *science*, 339(6127):1546–1558.
- Zhao, P. and Yu, B. (2006). On model selection consistency of lasso. *The Journal of Machine Learning Research*, 7:2541–2563.

Supplementary Materials for “PenPC: A Two-step Approach to Estimate the Skeletons of High Dimensional Directed Acyclic Graphs”

S.1 An example that neither covariance matrix nor concentration matrix captures the network skeleton

Consider a simple network of four nodes/variables X , Y , and Z and W , with the underlying network structure $X \rightarrow W \leftarrow Z \leftarrow Y$, and we assume there is no any other (hidden) variables. For illustration purpose, we assume the observations of these four random variables are generated through the following mechanism.

$$X = \epsilon_1, Y = \epsilon_2, Z = Y + \epsilon_3, \text{ and } W = X + Z + \epsilon_4 \quad (\text{S1})$$

where ϵ_j are i.i.d. $N(0, 1)$ for $1 \leq j \leq 4$. Denote the covariance matrix and partial covariance matrix of this system as Σ and Ω , respectively. Note $\Omega = \Sigma^{-1}$, and (i, j) -th entry of Ω indicates the covariance of the i -th and the j -th variables, conditioning on all the other covariates in this system. Let the connection matrix (i.e., skeleton)

of this system be Ξ . Then we have:

$$\Sigma = \begin{matrix} & \begin{matrix} X & Y & Z & W \end{matrix} \\ \begin{matrix} X \\ Y \\ Z \\ W \end{matrix} & \begin{pmatrix} 1 & 0 & 0 & 1 \\ 0 & 1 & 1 & 1 \\ 0 & 1 & 2 & 2 \\ 1 & 1 & 2 & 4 \end{pmatrix} \end{matrix}, \Omega = \begin{matrix} & \begin{matrix} X & Y & Z & W \end{matrix} \\ \begin{matrix} X \\ Y \\ Z \\ W \end{matrix} & \begin{pmatrix} 2 & 0 & 1 & -1 \\ 0 & 2 & -1 & 0 \\ 1 & -1 & 2 & -1 \\ -1 & 0 & -1 & 1 \end{pmatrix} \end{matrix}, \Xi = \begin{matrix} & \begin{matrix} X & Y & Z & W \end{matrix} \\ \begin{matrix} X \\ Y \\ Z \\ W \end{matrix} & \begin{pmatrix} 1 & 0 & 0 & 1 \\ 0 & 1 & 1 & 0 \\ 0 & 1 & 1 & 1 \\ 1 & 0 & 1 & 0 \end{pmatrix} \end{matrix}.$$

We see that neither Σ nor Ω gives us the correct connection matrix of network structure $X \rightarrow W \leftarrow Z \leftarrow Y$.

S.2 The details of the PenPC algorithm

In this section, we describe the step 2 of PenPC algorithm. For any undirected graph $\mathbf{G} = (V, F_{\mathbf{G}})$, we define the following quantities:

- $\mathbf{A}_{\mathbf{G},i,j} = [\text{adj}(i, \mathbf{G}) \cup \text{adj}(j, \mathbf{G})] \setminus \{i, j\}$,
- $\mathbf{B}_{\mathbf{G},i,j} = [\text{adj}(i, \mathbf{G}) \cap \text{adj}(j, \mathbf{G})] \setminus \{i, j\}$, and
- $\mathbf{C}_{\mathbf{G},i,j} = \{k : k \in \mathbf{A}_{i,j} \cap (\mathbf{B}_{\mathbf{G},i,j} \cup \text{Con}_{\mathbf{G}}^{(i,j)}(\mathbf{B}_{\mathbf{G},i,j}))\}$, where $\text{Con}_{\mathbf{G}}^{(i,j)}(\mathbf{B}_{\mathbf{G},i,j})$ is the set of vertices connected to any vertex in $\mathbf{B}_{\mathbf{G},i,j}$ by a chain of any length from a subgraph of \mathbf{G} , which is created by removing vertices i and j as well as any edges connected to i or j .

Then the algorithm is as follows.

Input: GGM $\mathcal{C}_{\mathcal{G}} = (V, F_{\mathcal{G}})$, which is obtained from the first step of the PenPC algorithm.

Output: Skeleton $\mathcal{G}^u = (V, E^u)$ and separation set $S(i, j)$ for edges $i - j \notin E^u$ but $i - j \in F_{\mathcal{G}}$.

1. **Set** $l = -1$ and $\mathbf{G} = (V, F_{\mathbf{G}}) = \mathcal{C}_{\mathcal{G}}$, i.e., $F_{\mathbf{G}} = F_{\mathcal{G}}$.
2. **For** any edge $i - j \in F_{\mathbf{G}}$,
 - 2.1 If X_i and X_j are marginally independent, then
 - delete edge $i - j$ from $F_{\mathbf{G}}$, and
 - set $S(i, j) = \emptyset$.
3. **Repeat:** $l = l+1$
 - 3.1 $\tilde{\mathbf{G}} = \mathbf{G}$
 - 3.2 **For** any edge $i - j \in F$ such that $|\mathbf{C}_{\tilde{\mathbf{G}}, i, j}| \geq l$.
 - 3.2.1 **Repeat:** Select $\Gamma \subseteq \mathbf{C}_{\tilde{\mathbf{G}}, i, j}$ with $|\Gamma| = l$.
 - 3.2.1.1 Set $\mathcal{K} = \mathbf{A}_{\tilde{\mathbf{G}}, i, j} \setminus \Gamma$.
 - 3.2.1.2 If X_i and X_j are conditionally independent given $\{X_k : k \in \mathcal{K}\}$, then
 - delete edge $i - j$ from $F_{\mathbf{G}}$, and
 - $S(i, j) = \mathcal{K}$.
 - 3.2.2 **Until:** The edge $i - j$ is deleted or all Γ with $|\Gamma| = l$ have been examined.
4. **Until:** for each $i - j \in F_{\mathbf{G}}$, $|\mathbf{C}_{\mathbf{G}, i, j}| < l$.
5. **Set** $\mathcal{G}^u = (V, E^u) = \mathbf{G}$, i.e., $E^u = F_{\mathbf{G}}$.

Figure S1: The second step of the PenPC algorithm. In steps 3.1-3.2, we save the current graph \mathbf{G} to $\tilde{\mathbf{G}}$, and all the conditional independence tests are based on $\tilde{\mathbf{G}}$ while \mathbf{G} is being updated. This is the “stable” part of the PC-stable algorithm, so that the order of the edges being tested does not matter.

S.3 The deterministic rules to extend a skeleton to a CPDAG

These deterministic rules have been described in Kalisch and Bühlmann (2007) and Pearl (2009). Given the skeleton \mathcal{G}^u and the separation sets $S(i, j)$ for all missing edges between nodes i and j , the arrow orientation of the skeleton proceeds in two step: (1) determination of the v -structure and (2) completion of the partially directed graph (PDAG).

step 1 For each pair of nonadjacent vertices i and j with common neighbor k , add arrow heads pointing at k , $i \rightarrow k \leftarrow j$ if $k \notin S(i, j)$.

step 2 In the PDAG from step 1, following four rules are repeatedly applied to obtain maximally oriented pattern.

rule 1: Orient $j - k$ into $j \rightarrow k$ whenever there is an arrow $i \rightarrow j$ such that i and k are nonadjacent.

rule 2: Orient $i - j$ into $i \rightarrow j$ whenever there is a chain $i \rightarrow k \rightarrow j$.

rule 3: Orient $i - j$ into $i \rightarrow j$ whenever there are two chains $i - k_1 \rightarrow j$ and $i - k_2 \rightarrow j$ such that k_1 and k_2 are nonadjacent.

The repeated application of these rules results in orienting all arrows that are common for all the DAGs within the same Markov equivalent class.

S.4 Supplementary Figures

Figure S2: Histograms of the degree ν under BA model with $p = 1000$ and $e = 2$ and the \log_{10} scale density of $\log_{10} \nu$ in the subplot.

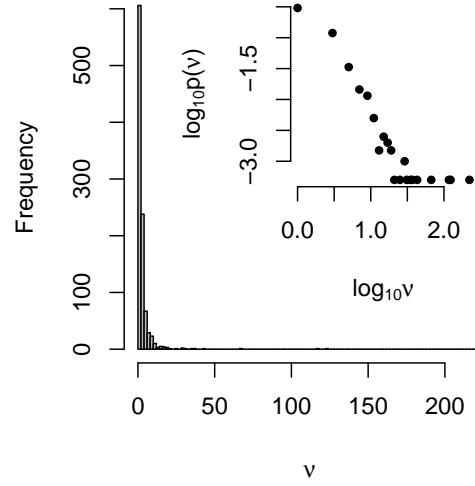


Figure S3: ER model ($p = 11, n = 100, p_E = 0.2$)

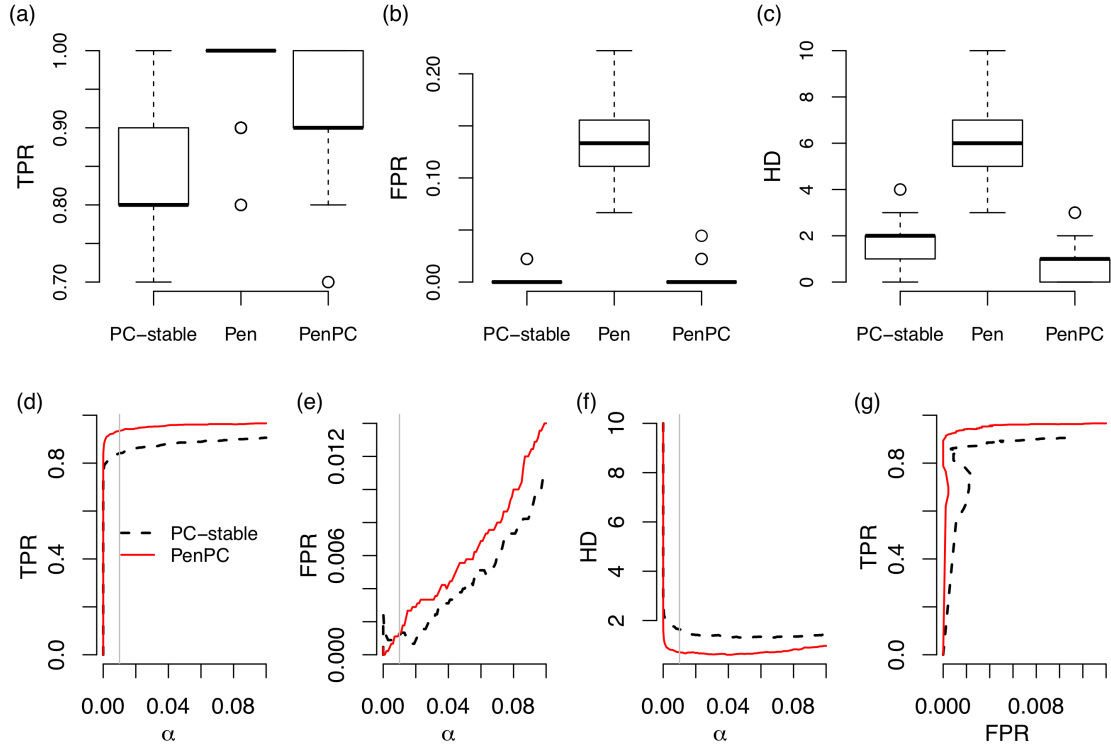


Figure S4: ER model ($p = 100, n = 30, p_E = 0.02$)

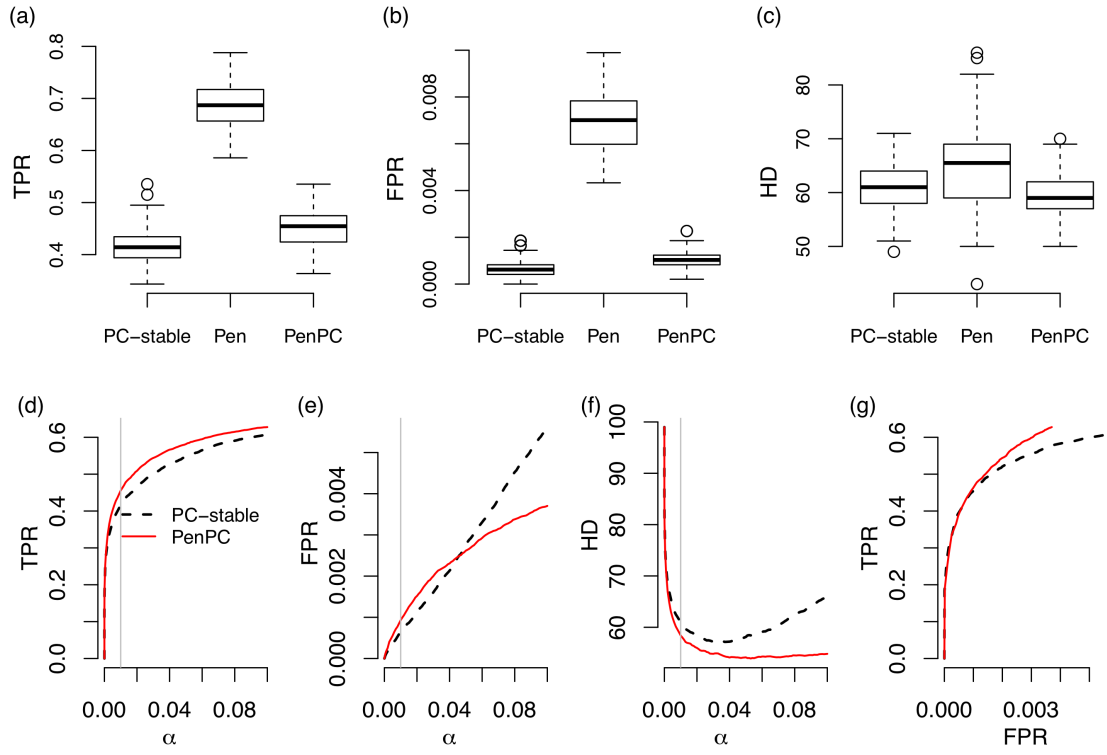


Figure S5: ER model ($p = 100, n = 30, p_E = 0.03$)

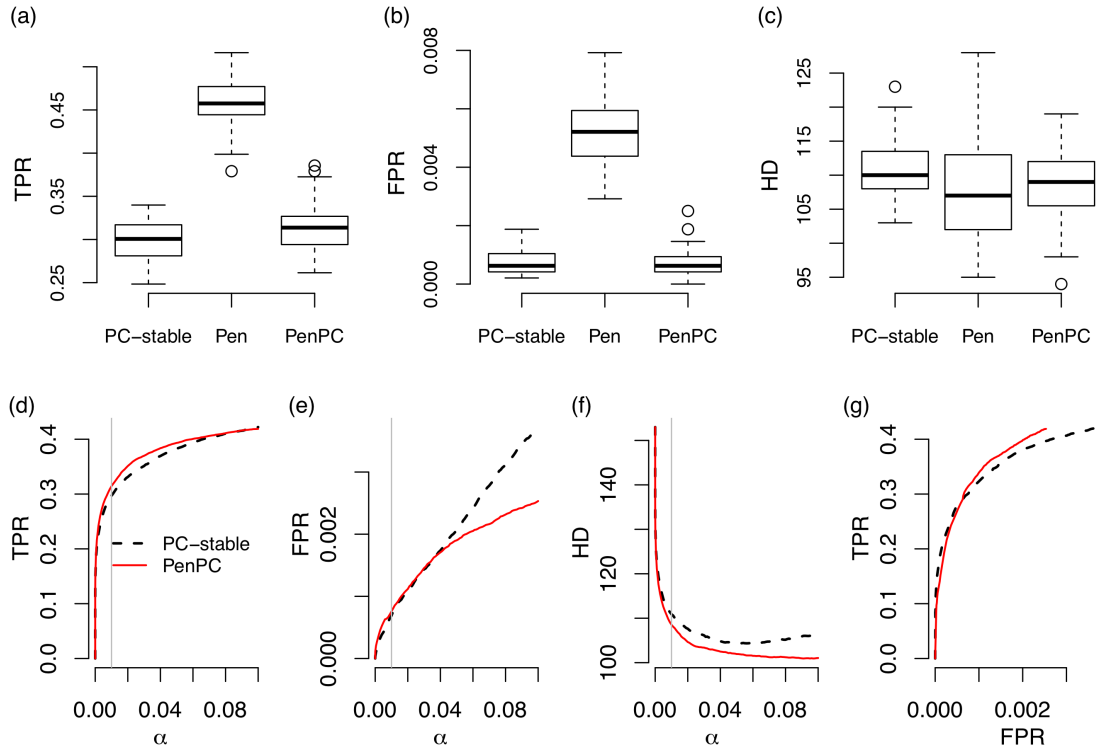


Figure S6: ER model ($p = 100, n = 30, p_E = 0.04$)

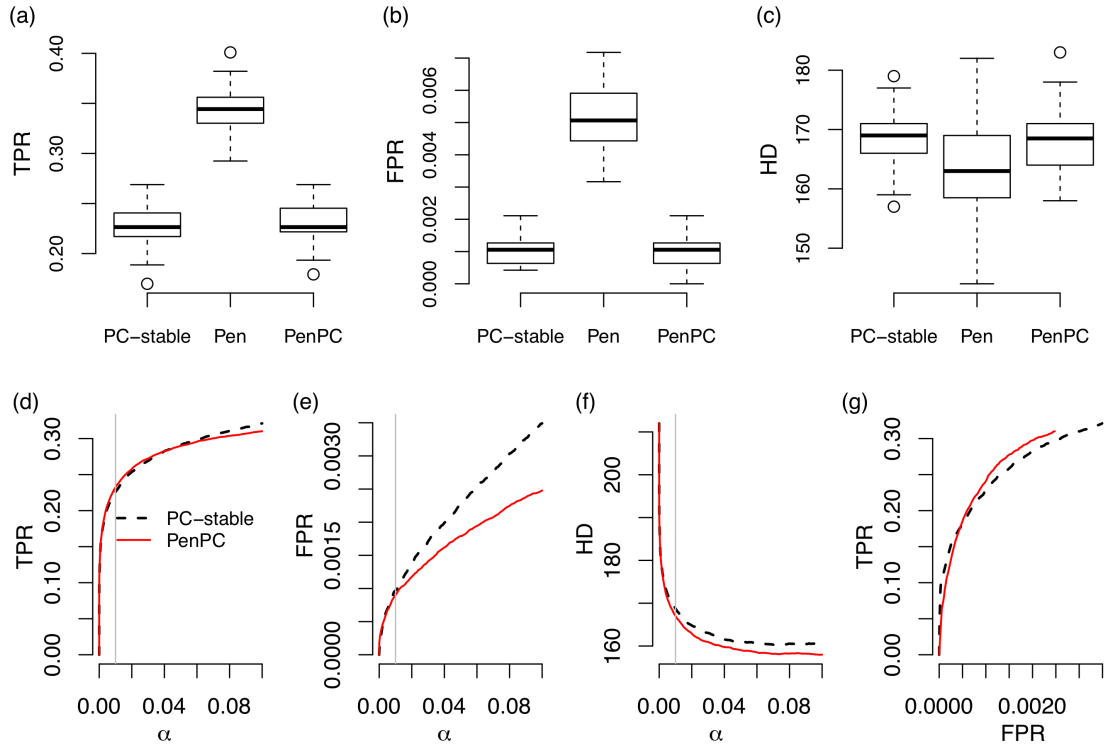


Figure S7: ER model ($p = 100, n = 30, p_E = 0.05$)

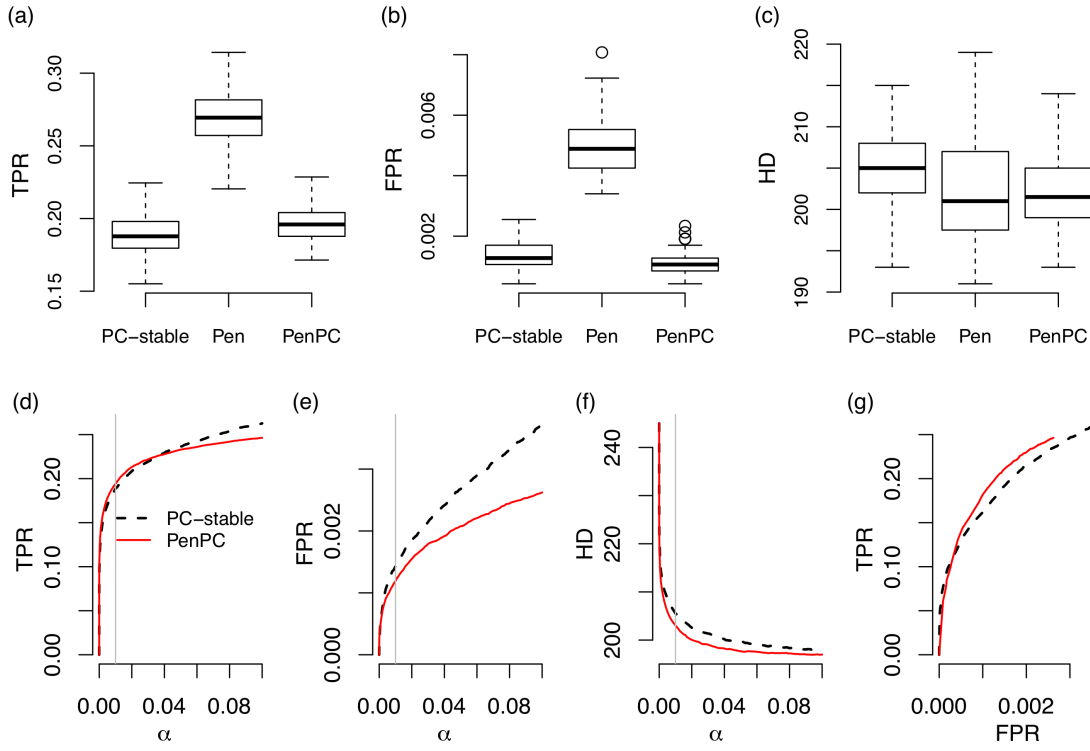


Figure S8: ER model ($p = 1000, n = 300, p_E = 0.002$)

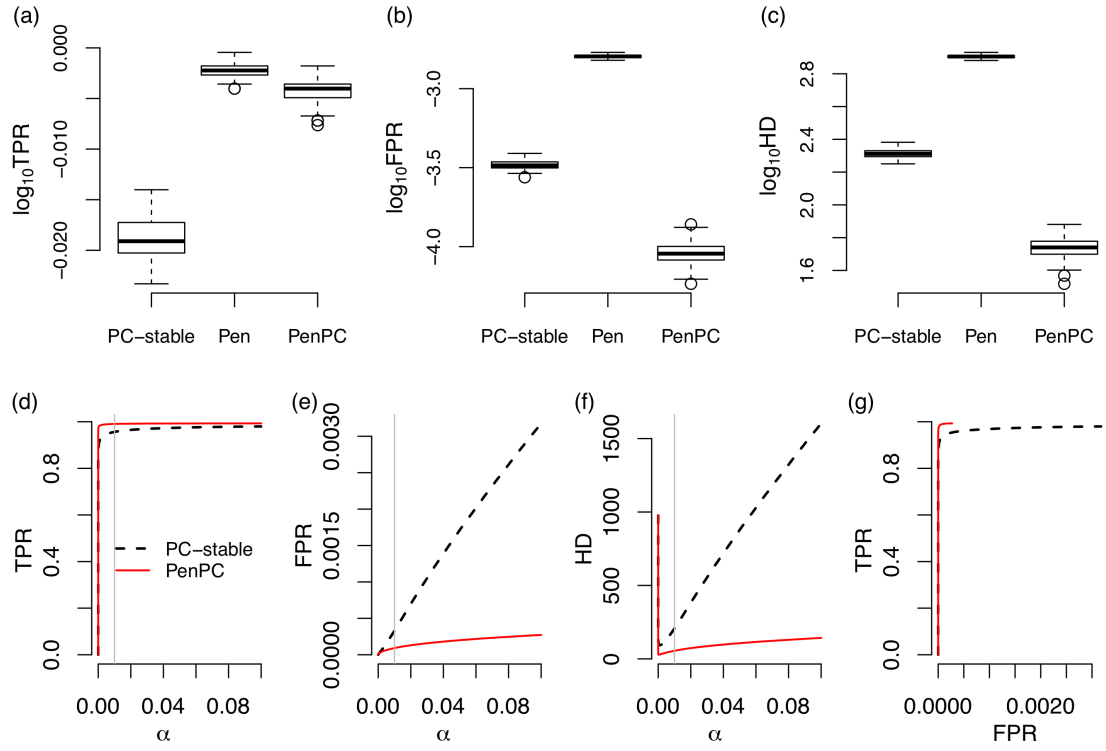


Figure S9: ER model ($p = 1000, n = 300, p_E = 0.01$)

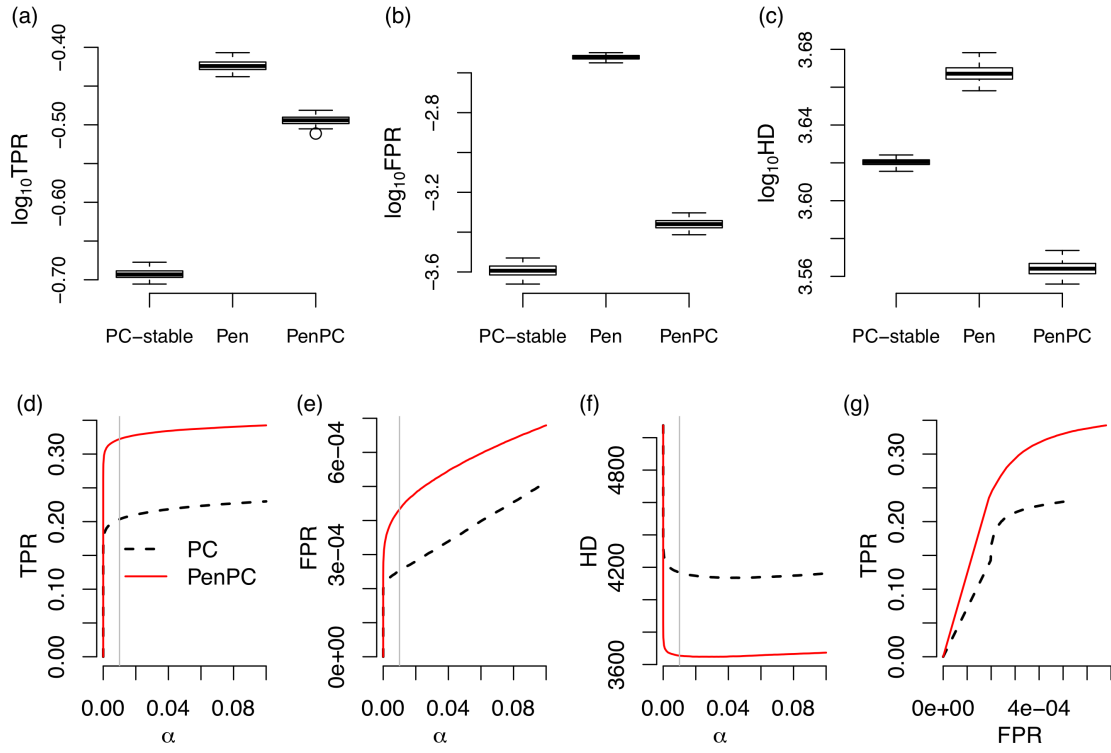


Figure S10: BA model ($p = 11, n = 100, e = 1$)

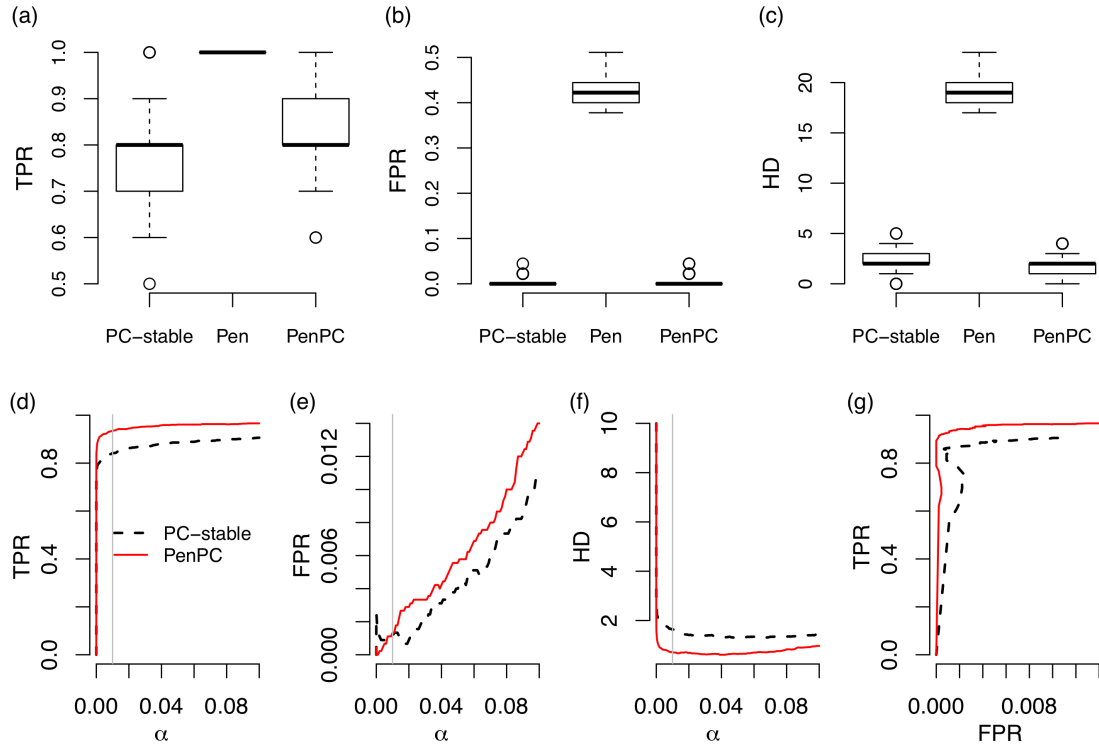


Figure S11: BA model ($p = 11, n = 100, e = 2$)

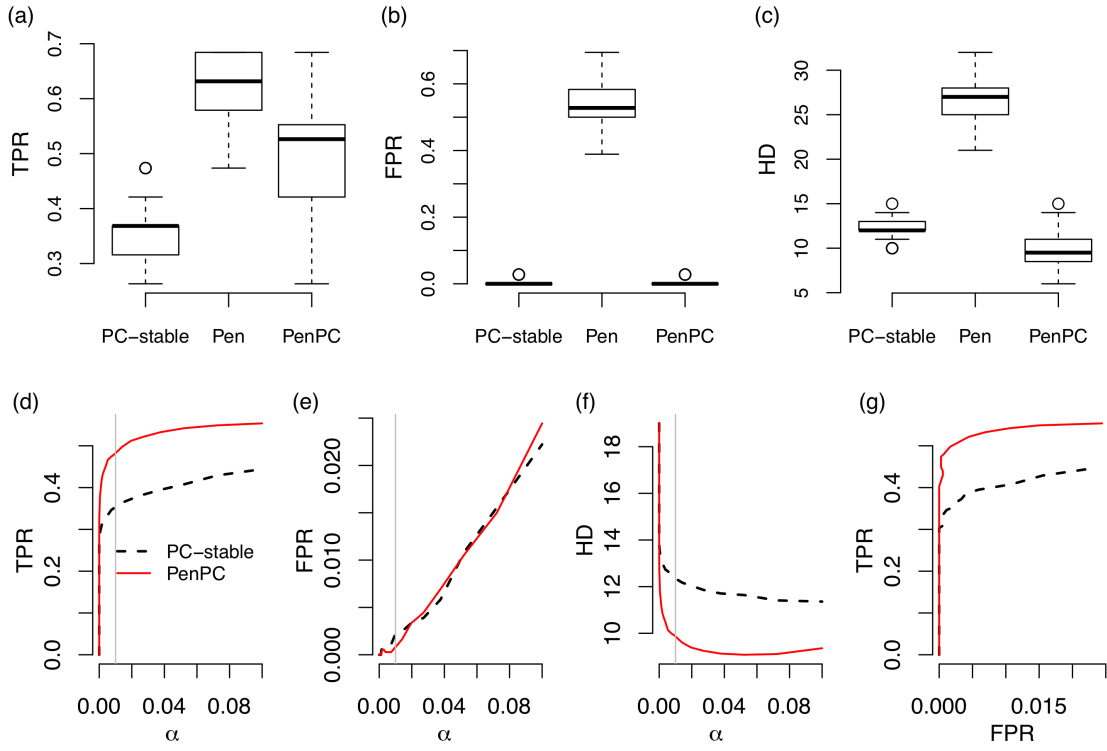


Figure S12: BA model ($p = 100, n = 30, e = 1$)

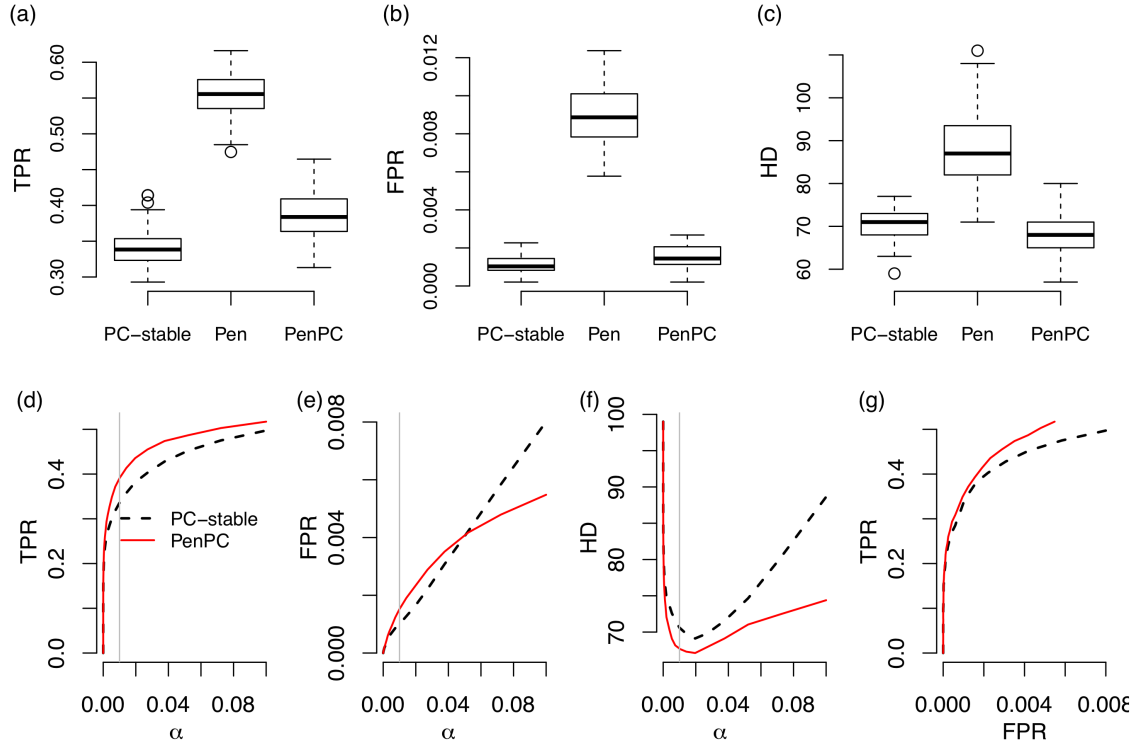


Figure S13: BA model ($p = 100, n = 30, e = 2$)

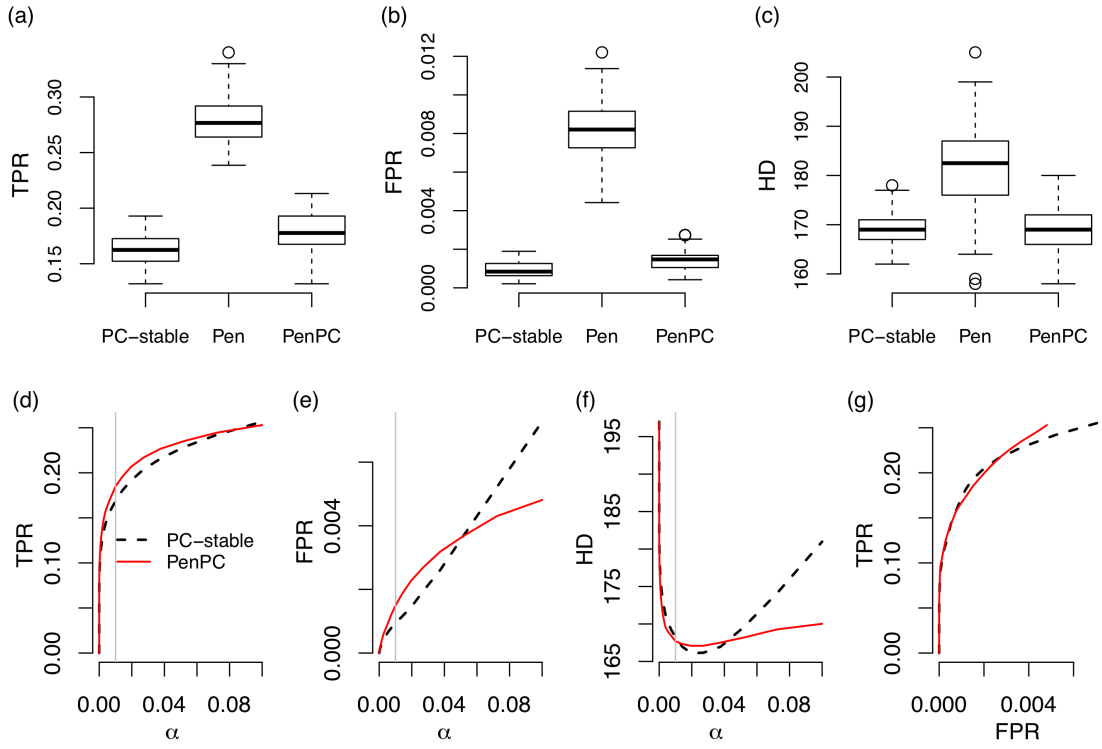


Figure S14: BA model ($p = 1000, n = 300, e = 1$)

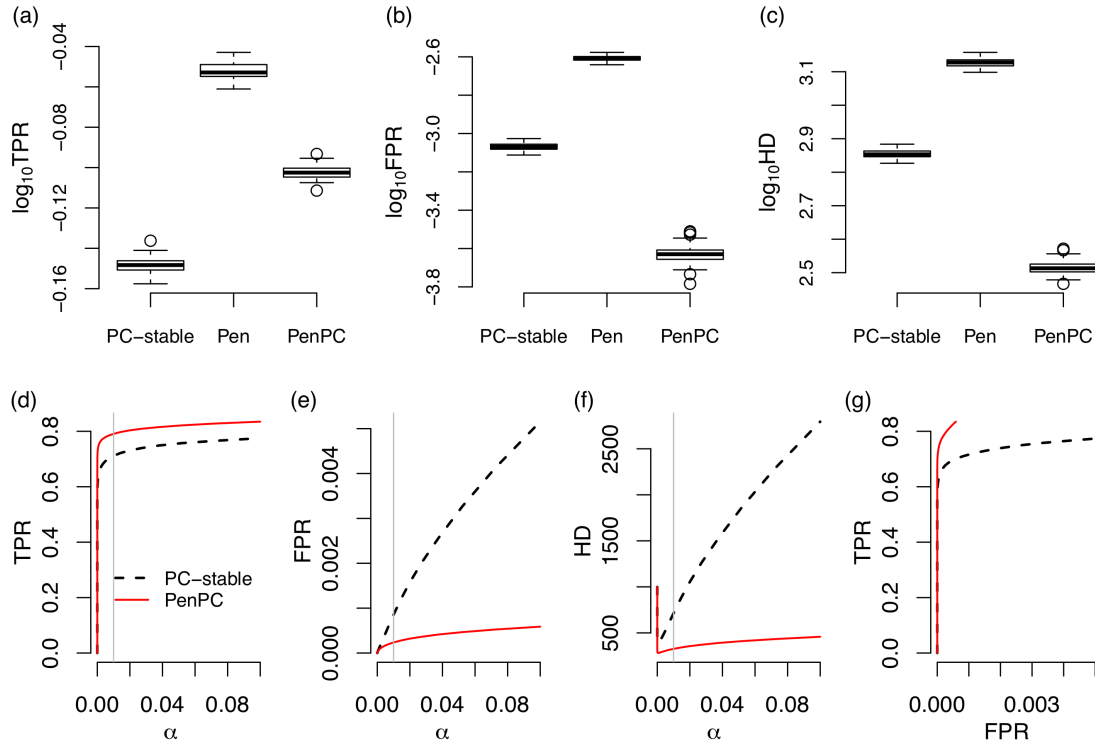
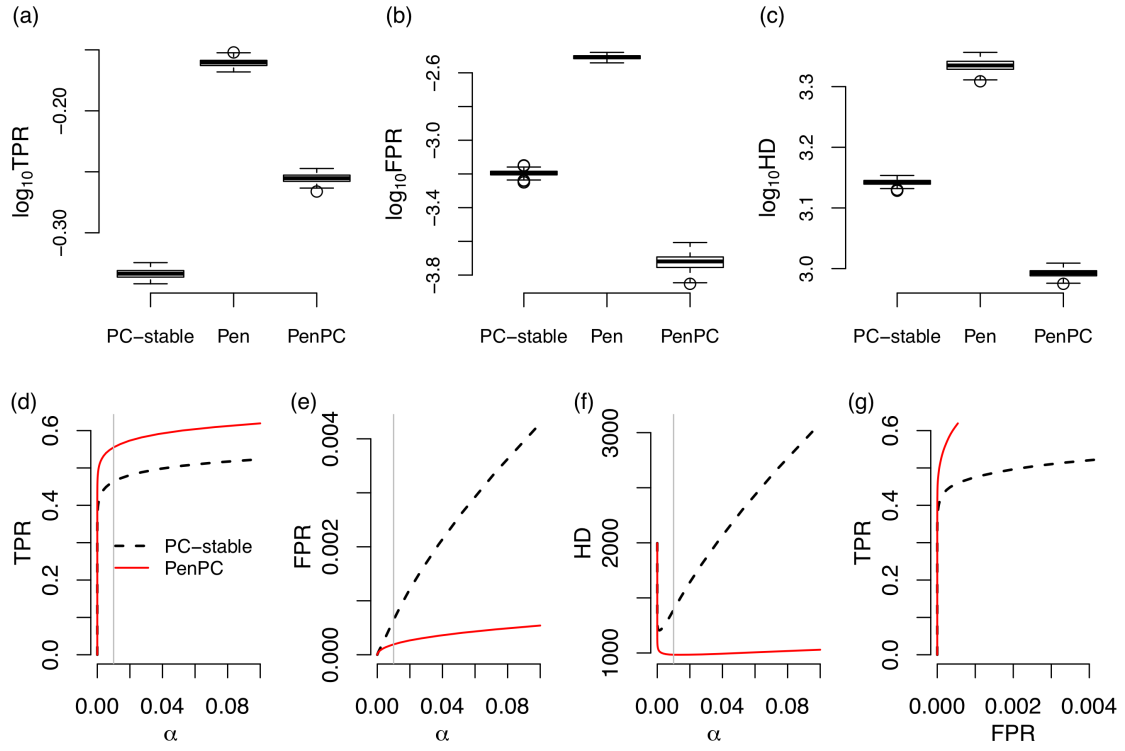


Figure S15: BA model ($p = 1000, n = 300, e = 2$)



S.5 Proofs

S.5.1 Lemma 5

The following lemma is needed for proof of Theorem 1. It provides a sufficient condition for strict local minimizer $\hat{\mathbf{b}}_i$ of equation (3) in the main text.

Lemma 5: Assume that $p(t; \lambda, \tau) = \lambda \rho(t; \tau)$ satisfies Condition 1. Define $\bar{\rho}(t; \tau) = \text{sgn}(t) \rho'(|t|; \tau)$, $t \in \mathbb{R}$ and $\bar{\rho}(\mathbf{t}; \tau) = (\bar{\rho}(t_1; \tau), \dots, \bar{\rho}(t_q; \tau))^T$, $\mathbf{t} = (t_1, \dots, t_q)^T$. Then $\hat{\mathbf{b}}_i \in \mathbb{R}^{p_n-1}$ is a strict local minimizer of

$$Q(\mathbf{b}_i) = \frac{1}{2}(\mathbf{x}_i - \mathbf{X}_{-i}\mathbf{b}_i)^T(\mathbf{x}_i - \mathbf{X}_{-i}\mathbf{b}_i) + n \sum_{j \neq i} p(|b_{i,j}|; \lambda_i, \tau_i)$$

if

$$\mathcal{X}_{i1}^T(\mathbf{x}_i - \mathbf{X}_{-i}\hat{\mathbf{b}}_i) = n\lambda_i\bar{\rho}(\hat{\mathbf{b}}_{i1}; \tau_i), \quad (\text{S2})$$

$$\|\mathcal{X}_{i2}^T(\mathbf{x}_i - \mathbf{X}_{-i}\hat{\mathbf{b}}_i)\|_\infty < p'(0+; \lambda_i, \tau_i), \quad (\text{S3})$$

$$\|(\mathcal{X}_{i1}^T \mathcal{X}_{i1})^{-1}\|_2 < 1/(n\kappa(\hat{\mathbf{b}}_{i1}; \lambda_i, \tau_i)), \quad (\text{S4})$$

where $\kappa(\mathbf{v}; \lambda_i, \tau_i) = \lim_{\epsilon \rightarrow 0+} \max_{1 \leq j \leq r} \sup_{t_1 < t_2 \in (|v_j|-\epsilon, |v_j|+\epsilon)} -\frac{p'(t_2; \lambda_i, \tau_i) - p'(t_1; \lambda_i, \tau_i)}{t_2 - t_1}$ for any vector $\mathbf{v} = (v_1, \dots, v_r)^T \in \mathbb{R}^r$, $\hat{\mathbf{b}}_{i1}$ is the subvector of $\hat{\mathbf{b}}_i$'s nonzero components. On the other hand, if $\hat{\mathbf{b}}_i$ is a local maximizer of $Q(\mathbf{b}_i)$, then it must satisfy (2)-(4) with strict inequalities replaced by non-strict inequalities.

Lemma 5 is a special case of the Theorem 1 in Fan and Lv (2011) and thus we skip the proof.

S.5.2 Proof of Theorem 1

For any fixed $i \in V_n$, \mathbf{x}_i is a $n \times 1$ response vector and \mathbf{X}_{-i} is a $n \times q$ covariate matrix with $q = p_n - 1$ corresponding to vertices $V_n \setminus \{i\}$. Let $\mathcal{S}_i = \text{supp}(\mathbf{b}_i)$ to be the support of the true regression coefficient \mathbf{b}_i with $|\mathcal{S}_i| = s_i$. Define $\boldsymbol{\xi}_i = (\xi_{i1}, \dots, \xi_{iq})^\top = \mathbf{X}_{-i}^\top (\mathbf{x}_i - \mathbf{X}_{-i} \mathbf{b}_i) = \mathbf{X}_{-i}^\top \boldsymbol{\epsilon}_i$ where $\boldsymbol{\epsilon}_i \sim N_n(0, \sigma_i^2 I_n)$ for $n \times n$ identity matrix I_n . Let $\boldsymbol{\xi}_{i1}$ and $\boldsymbol{\xi}_{i2}$ to be the non-joint sub-vectors with indices partitioned by \mathcal{S}_i . Define the event

$$\mathcal{E}_i = \left\{ \|\boldsymbol{\xi}_i\|_\infty \leq \sigma_i n^{1/2+a/2} \sqrt{\log(n)} \right\}. \quad (\text{S5})$$

We first consider the property of penalized regression on \mathcal{E}_i . Lemma 5 gives sufficient conditions of a local minimizer. We prove that within the hypercube

$$\mathcal{N}_i = \{\boldsymbol{\beta} = (\boldsymbol{\beta}_1^\top, \boldsymbol{\beta}_2^\top)^\top \in \mathbb{R}^q : \|\boldsymbol{\beta}_1 - \mathbf{b}_{i1}\|_\infty \leq Cn^{-d_2}, \boldsymbol{\beta}_2 = \mathbf{0}\}, \quad (\text{S6})$$

there is a solution $\hat{\mathbf{b}}_i$ that satisfy (2) and (3), and equation (4) of Lemma 5 holds by Assumption (A5).

Step 1: Find a solution to (2) in \mathcal{N}_i .

We will prove that conditioning on \mathcal{E}_i , there is a solution $\hat{\mathbf{b}}_{i1} \in \mathbb{R}^{s_i}$ for equation (2) of Lemma 5 which is equivalent to

$$\hat{\mathbf{b}}_{i1} = \mathbf{b}_{i1} + (\mathcal{X}_{i1}^\top \mathcal{X}_{i1})^{-1} \{ \mathcal{X}_{i1}^\top \boldsymbol{\epsilon} - n\lambda_i \bar{\rho}(\hat{\mathbf{b}}_{i1}; \tau_i) \}.$$

Suppose that $\boldsymbol{\beta} = (\boldsymbol{\beta}_1^\top, \boldsymbol{\beta}_2^\top)^\top \in \mathbb{R}^q$ has the same partition as $\mathbf{b}_i = (\mathbf{b}_{i1}^\top, \mathbf{b}_{i2}^\top)^\top$. Let $\mathbf{u}_i = (\mathcal{X}_{i1}^\top \mathcal{X}_{i1})^{-1} [\mathcal{X}_{i1}^\top \boldsymbol{\epsilon} - n\lambda_i \bar{\rho}(\boldsymbol{\beta}_1; \tau_i)]$, and $\phi(\boldsymbol{\beta}_1) = \boldsymbol{\beta}_1 - \mathbf{b}_{i1} - \mathbf{u}_i$, where $\boldsymbol{\beta}_1 = (\beta_{1,1}, \dots, \beta_{1,s_i})^\top \in \mathbb{R}^{s_i}$ and $\mathbf{b}_{i1} = (b_{i1,1}, \dots, b_{i1,s_i}) \in \mathbb{R}^{s_i}$. It suffices to show that there is a solution to $\phi(\boldsymbol{\beta}_1) = \mathbf{0}$ in \mathcal{N}_i . Suppose $\|\mathbf{u}_i\|_\infty = o(n^{-d_2})$. For sufficiently large

n , if $\beta_{1,j} - b_{i1,j} = Cn^{-d_2}$, $\phi_j(\boldsymbol{\beta}_1) \geq Cn^{-d_2} - \|\mathbf{u}_i\|_\infty > 0$. If $\beta_{1,j} - b_{i1,j} = -Cn^{-d_2}$, $\phi_j(\boldsymbol{\beta}_1) \leq -Cn^{-d_2} + \|\mathbf{u}_i\|_\infty < 0$. By the continuity of function $\phi(\boldsymbol{\beta}_1)$ and Miranda's existence theorem, there is a solution for $\phi(\boldsymbol{\beta}_1) = \mathbf{0}$ in \mathcal{N}_i .

Now we prove $\|\mathbf{u}_i\|_\infty = o(n^{-d_2})$. For any $\boldsymbol{\beta} = (\boldsymbol{\beta}_1^T, \boldsymbol{\beta}_2^T)^T \in \mathcal{N}_i$, $|\beta_{1,j}| \geq |b_{i1,j}| - \delta_n$ where δ_n is defined in Assumption (A3), and thus

$$\min_{j=1,\dots,s_i} |\beta_{1,j}| \geq \min_{j=1,\dots,s_i} |b_{i1,j}| - \delta_n \geq \delta_n.$$

By monotonicity of $\rho(t; \tau)$ in Condition 1, $\|\bar{\rho}(\boldsymbol{\beta}_1; \tau_i)\|_\infty \leq \rho'(\delta_n; \tau_i)$. Therefore, on \mathcal{E}_i ,

$$\|\mathcal{X}_{i1}^T \boldsymbol{\epsilon} - n\lambda_i \bar{\rho}(\boldsymbol{\beta}_1; \tau_i)\|_\infty \leq \sigma_i n^{1/2+a/2} \sqrt{\log(n)} + np'(\delta_n; \lambda_i, \tau_i).$$

Then by Assumption (A5),

$$\|\mathbf{u}_i\|_\infty \leq \sigma_i n^{-1/2+a/2+s_0} \sqrt{\log(n)} + n^{s_0} p'(\delta_n; \lambda_i, \tau_i).$$

By Assumption (A3), $\sigma_i n^{-1/2+a/2+s_0} \sqrt{\log(n)} = o(n^{-d_2})$ and by Assumption (A4), $n^{s_0} p'(\delta_n; \lambda_i, \tau_i) = o(n^{-d_2})$. Therefore, $\|\mathbf{u}_i\|_\infty = o(n^{-d_2})$.

Step 2: Verify Condition (3) holds for $\hat{\mathbf{b}}_i$.

For $\hat{\mathbf{b}}_i \in \mathcal{N}_i$ satisfying the condition (3), we need to verify

$$\|\mathcal{X}_{i2}^T(\mathbf{x}_i - \mathbf{X}_{-i}\hat{\mathbf{b}}_i)\|_\infty < np'(0+; \lambda_i, \tau_i)$$

on the event \mathcal{E}_i . Note that

$$\mathcal{X}_{i2}^T(\mathbf{x}_i - \mathbf{X}_{-i}\hat{\mathbf{b}}_i) = \mathcal{X}_{i2}^T(\mathbf{x}_i - \mathbf{X}_{-i}\mathbf{b}_i) - \mathcal{X}_{i2}^T(\mathbf{X}_{-i}\hat{\mathbf{b}}_i - \mathbf{X}_{-i}\mathbf{b}_i) = \boldsymbol{\xi}_{i2} - \mathcal{X}_{i2}^T \mathcal{X}_{i1}(\hat{\mathbf{b}}_{i1} - \mathbf{b}_{i1}).$$

By Condition 1, $\|\rho'(\hat{\mathbf{b}}_{i1}; \tau_i)\|_\infty \leq \rho'(\delta_n; \tau_i)$. On \mathcal{E}_i , by Assumptions (A4) and (A5) we

have

$$\begin{aligned}
& \|\mathcal{X}_{i2}^T(\mathbf{x}_i - \mathbf{X}_{-i}\hat{\mathbf{b}}_i)\|_\infty \\
& \leq \|\boldsymbol{\xi}_{i2}\|_\infty + \|\mathcal{X}_{i2}^T \mathcal{X}_{i1}(\hat{\mathbf{b}}_{i1} - \mathbf{b}_{i1})\|_\infty \\
& \leq \sigma_i n^{1/2+a/2} \sqrt{\log(n)} + \|\mathcal{X}_{i2}^T \mathcal{X}_{i1}(\mathcal{X}_{i1}^T \mathcal{X}_{i1})^{-1}\|_\infty \left[\|\boldsymbol{\xi}_{i1}\|_\infty + n\|p'(\hat{\mathbf{b}}_{i1}; \lambda_i, \tau_i)\|_\infty \right] \\
& \leq \sigma_i n^{1/2+a/2+b} \sqrt{\log(n)} + Knp'(0+; \lambda_i, \tau_i) \\
& < np'(0+; \lambda_i, \tau_i)
\end{aligned}$$

for sufficiently large n .

Step 3: Prove that $\mathbb{P}(\mathcal{E}_i) > 1 - C \exp\{n^a - n^a \log(n)/2\}$.

Since $\|\mathbf{x}_i\|_2 = \sqrt{n}$, $(\sqrt{n}\sigma_i)^{-1}\xi_{ij} \sim N(0, 1)$. We have

$$\begin{aligned}
\mathbb{P}(\mathcal{E}_i) & \geq 1 - \sum_{j=1}^q \mathbb{P}\left\{(\sqrt{n}\sigma_i)^{-1}|\xi_{ij}| > n^{a/2} \sqrt{\log(n)}\right\} \\
& > 1 - Cp \exp\left(-\frac{n^a}{2} \log(n) - \frac{a}{2} \log(n) - \log \log(n)\right) \\
& > 1 - C \exp\{n^a - n^a \log(n)/2\}.
\end{aligned}$$

The last inequality is due to Assumption (A1).

S.5.3 Proof of Corollary 1

Let $\mathcal{E} = \bigcap_{i=1}^{p_n} \mathcal{E}_i$ where \mathcal{E}_i defined in (5). Therefore $\mathbb{P}(\mathcal{E}) \geq 1 - \sum_{i=1}^{p_n} (1 - \mathbb{P}(\mathcal{E}_i)) \geq 1 - C \exp\{2n^a - n^a \log(n)/2\} \rightarrow 1$.

S.5.4 Proof of Lemma 3

Suppose that two vertices i and j are not connected in the skeleton \mathcal{G}_n^u , but connected in the GGM $\mathcal{C}_{\mathcal{G}_n}$. In addition, they are not marginally independent. By Lemma 2, there exists at least one vertex k such that $i \rightarrow k \leftarrow j$. Let $\text{adj}_j(i, \mathcal{C}_{\mathcal{G}_n}) = \text{adj}(i, \mathcal{C}_{\mathcal{G}_n}) \setminus j$. Let $\text{ch}_{\mathcal{G}_n}(i)$ and $\text{de}_{\mathcal{G}_n}(i)$ be the sets of children and descendants of i in \mathcal{G}_n . Let $\text{ch}_{\mathcal{G}_n}(i, j) = \text{ch}_{\mathcal{G}_n}(i) \cap \text{ch}_{\mathcal{G}_n}(j)$, i.e., the common children of i and j . Let $\pi_i = \text{adj}_j(i, \mathcal{C}_{\mathcal{G}_n}) \setminus \left[\bigcup_{v \in \text{ch}_{\mathcal{G}_n}(i, j)} (\{v\} \cup \text{de}_{\mathcal{G}_n}(v)) \right]$ and $\pi_j = \text{adj}_i(j, \mathcal{C}_{\mathcal{G}_n}) \setminus \left[\bigcup_{v \in \text{ch}_{\mathcal{G}_n}(i, j)} (\{v\} \cup \text{de}_{\mathcal{G}_n}(v)) \right]$. We show that i and j is d-separated by $\pi_i \cup \pi_j$ and $\pi_i \cup \pi_j \in \Pi_{i, j}$.

In order to show that $i \perp\!\!\!\perp j | (\pi_i \cup \pi_j)$, we consider a sequence of vertices k_1, \dots, k_m for $m \geq 1$ of chains such that

$$\text{(Chain 1)} \quad i \rightarrow k_1 - \dots - k_m \leftarrow j,$$

$$\text{(Chain 2)} \quad i \rightarrow k_1 - \dots - k_m \rightarrow j,$$

$$\text{(Chain 3)} \quad i \leftarrow k_1 - \dots - k_m \leftarrow j,$$

$$\text{(Chain 4)} \quad i \leftarrow k_1 - \dots - k_m \rightarrow j.$$

These four cases cover all possible chains connecting i and j while we allow k_1 and k_m to be the same. It suffices to show that $\pi_i \cup \pi_j$ blocks all the four types of chains between i and j . For the (Chain 2), a set including the arrow emitting vertex k_m d-separates i and j by Definition 1 on d-separation. Since $k_m \in \text{adj}_i(j, \mathcal{C}_{\mathcal{G}_n})$ and $k_m \notin \text{ch}_{\mathcal{G}_n}(j)$ because of no loop restriction, $k_m \in \pi_i \cup \pi_j$. Similarly for the (Chain 3), since the arrow emitting vertex $k_1 \in \text{adj}_j(i, \mathcal{C}_{\mathcal{G}_n})$ but $k_1 \notin \text{ch}_{\mathcal{G}_n}(i)$, $k_1 \in \pi_i \cup \pi_j$. The (Chain 4) also blocked by either arrow-emitting vertices k_1 or k_2 included in $\pi_i \cup \pi_j$. In the (Chain 1), there must be at least one collider. If $m = 1$, then k_m is a common child so that it is excluded from $\pi_i \cup \pi_j$. If $m = 2$, the possible

chains are $i \rightarrow k_1 \rightarrow k_2 \leftarrow j$ or $i \rightarrow k_1 \leftarrow k_2 \leftarrow j$ and both chains have one arrow emitting vertex, k_1 or k_2 in $\pi_i \cup \pi_j$. Now we suppose that there are at least three vertices, $m > 2$. If at least one of k_1 and k_m is not a collider, there exists a arrow emitting vertex in $\pi_i \cup \pi_j$. If both k_1 and k_m are colliders, the (Chain 1) is $i \rightarrow k_1 \leftarrow k_2 \leftarrow \dots \leftarrow k_{m-1} \rightarrow k_m \leftarrow j$. Since the arrow emitting vertices k_2 and k_{m-1} are not in $\text{ch}_{\mathcal{G}_n}(i) \cap \text{ch}_{\mathcal{G}_n}(j)$ but in $\text{adj}_j(i, \mathcal{C}_{\mathcal{G}_n}) \cup \text{adj}_i(j, \mathcal{C}_{\mathcal{G}_n})$, those are in $\pi_i \cup \pi_j$. Therefore, $\pi_i \cup \pi_j$ blocks all chains between i and j .

Next we need to prove $\pi_i \cup \pi_j \in \Pi_{i,j}$. Let $V_{n,-i,-j} = V_n \setminus \{i, j\}$. Since $\pi_i \cup \pi_j = [\text{adj}_j(i, \mathcal{C}_{\mathcal{G}_n}) \cup \text{adj}_i(j, \mathcal{C}_{\mathcal{G}_n})] \setminus \left[\bigcup_{v \in \text{ch}_{\mathcal{G}_n}(i,j)} (\{v\} \cup \text{de}_{\mathcal{G}_n}(v)) \right]$, it is obvious that

$$\bigcup_{v \in \text{ch}_{\mathcal{G}_n}(i,j)} (\{v\} \cup \text{de}_{\mathcal{G}_n}(v)) \subseteq \bigcup_{v \in \text{adj}(i,j, \mathcal{C}_{\mathcal{G}_n})} \text{Con}(v, \mathcal{C}_{\mathcal{G}_n}(V_{n,-i,-j})),$$

and thus $\pi_i \cup \pi_j \in \Pi_{i,j}$.

S.5.5 Lemma 6

We state Lemma 6 which is used to prove Theorem 2. This lemma is essentially the same as Lemma 3 in Kalisch and Bühlmann (2007). The proof is therefore skipped.

Lemma 6: Let $g(\rho) = 0.5 \log((1 + \rho)/(1 - \rho))$. Denote by $\hat{z}_{i,j|\mathcal{K}} = g(\hat{\rho}_{i,j|\mathcal{K}})$ and by $z_{i,j|\mathcal{K}} = g(\rho_{i,j|\mathcal{K}})$ where $\mathcal{K} \subseteq \text{adj}(i, \mathcal{C}_{\mathcal{G}_n}) \cup \text{adj}(j, \mathcal{C}_{\mathcal{G}_n})$. Assume the distribution of $X = (X_1, X_2, \dots, X_p)^T$ is multivariate Gaussian and $\sup_{i,j,\mathcal{K}} |\rho_{i,j|\mathcal{K}}| \leq M < 1$ (the second part of Assumption (A6)). Then, for any $0 < \gamma < 2$,

$$\sup_{i,j,\mathcal{K}} \mathbf{P}(|\hat{z}_{i,j|\mathcal{K}} - z_{i,j|\mathcal{K}}| > \gamma) \leq O(n - \nu_i - \nu_j) [\exp\{-(C_1 + C_2)(n - \nu_i - \nu_j - 4)\}],$$

where $\nu_i = |\text{adj}(i, \mathcal{C}_{\mathcal{G}_n})|$ and C_1 and C_2 are two positive constants. More specifically,

$$C_1 = \log \left[\frac{4 + (\gamma l)^2}{4 - (\gamma l)^2} \right], \quad C_2 = \log \left[\frac{16 + (1 - M)^2}{16 - (1 - M)^2} \right],$$

where $l = 1 - (1 + M)^2/4$.

S.5.6 Proof of Theorem 2

For an edge $i - j \in F_n$ of $\mathcal{C}_{\mathcal{G}_n}$, define \mathcal{K} to be any set in $\mathbf{\Pi}_{i,j}$ of (4) with $|\mathcal{K}| < n - 3$. Let $\nu_i = |\text{adj}(i, \mathcal{C}_{\mathcal{G}_n})|$ for all $i \in V_n$. From Lemma 5 in the Supplementary Materials, if $\gamma \rightarrow 0$, $C_1 \sim (\gamma l)^2/2 \rightarrow 0$. In contrast, C_2 is a constant. Therefore the term $\exp\{-C_2(n - \nu_i - \nu_j - 4)\}$ is negligible, and thus

$$\begin{aligned} \sup_{i,j,\mathcal{K}} \mathbb{P}(|\hat{z}_{i,j|\mathcal{K}} - z_{i,j|\mathcal{K}}| > \gamma) &\leq O(n - \nu_i - \nu_j) \exp\{-(\gamma l)^2(n - \nu_i - \nu_j - 4)/2\} \\ &\leq O(n - \nu_i - \nu_j) \exp\{-C_3(n - \nu_i - \nu_j)\gamma^2\}, \end{aligned}$$

where C_3 is a constant.

Denote by $E_{i,j|\mathcal{K}}$ the event “an error occurred when testing partial correlation for zero at nodes i, j with conditional set \mathcal{K} ”. An error can be a type I error or a type II error, denoted by $E_{i,j|\mathcal{K}}^I$ and $E_{i,j|\mathcal{K}}^{II}$, respectively. Therefore $E_{i,j|\mathcal{K}} = E_{i,j|\mathcal{K}}^I \cup E_{i,j|\mathcal{K}}^{II}$, and

$$\begin{aligned} E_{i,j|\mathcal{K}}^I &: \sqrt{n - |\mathcal{K}| - 3} |\hat{z}_{i,j|\mathcal{K}}| > \Phi^{-1}(1 - \alpha/2) \text{ and } z_{i,j|\mathcal{K}} = 0, \\ E_{i,j|\mathcal{K}}^{II} &: \sqrt{n - |\mathcal{K}| - 3} |\hat{z}_{i,j|\mathcal{K}}| \leq \Phi^{-1}(1 - \alpha/2) \text{ and } z_{i,j|\mathcal{K}} \neq 0. \end{aligned}$$

Choose $\alpha = \alpha_n = 2(1 - \Phi(\sqrt{n}c_n/2))$, where c_n is defined in Assumption (A3).

Then

$$\begin{aligned} \sup_{i,j,\mathcal{K}} \mathbf{P}(E_{i,j|\mathcal{K}}^I) &= \sup_{i,j,\mathcal{K}} \mathbb{P} \left[|\hat{z}_{i,j|\mathcal{K}} - z_{i,j|\mathcal{K}}| > \sqrt{n/(n - |\mathcal{K}| - 3)} c_n/2 \right] \\ &\leq O(n - \nu_i - \nu_j) \exp \left[-C_4(n - \nu_i - \nu_j) c_n^2 \right], \end{aligned}$$

for some constant C_4 . With the same choice of α ,

$$\begin{aligned} \sup_{i,j,\mathcal{K}} \mathbb{P}(E_{i,j|\mathcal{K}}^{II}) &= \sup_{i,j,\mathcal{K}} \mathbb{P} \left[|\hat{z}_{i,j|\mathcal{K}}| \leq \sqrt{n/(n - |\mathcal{K}| - 3)} c_n/2 \right] \\ &\leq \sup_{i,j,\mathcal{K}} \mathbb{P} \left[|\hat{z}_{i,j|\mathcal{K}} - z_{i,j|\mathcal{K}}| > c_n \left(1 - \sqrt{n/(n - |\mathcal{K}| - 3)}/2 \right) \right] \\ &\leq O(n - \nu_i - \nu_j) \exp \left[-C_5(n - \nu_i - \nu_j) c_n^2 \right], \end{aligned}$$

for some constant C_5 .

$$\begin{aligned} &\mathbb{P}(\text{an error occurs in the step 2 of PenPC algorithm}) \\ &\leq \sum_{(i,j) \in F_n} 2^{\nu_i + \nu_j} O((n - \nu_i - \nu_j)) \exp \{ -C_6(n - \nu_i - \nu_j) c_n^2 \} \\ &\leq O \left[\sum_{i=1}^{p_n} \sum_{j \in \text{adj}(i, \mathcal{C}_{\mathcal{G}_n})} n 2^{2q_n} \exp \{ -C_6(n - 2q_n) c_n^2 \} \right] \\ &\leq O \left[np_n q_n \exp \{ 2q_n - C_6(n - 2q_n) c_n^2 \} \right] \\ &\leq O \left[np_n q_n \exp \{ -C_6 n^{1-2d_1} + C_7 q_n \} \right] \tag{S7} \\ &\leq O \left[n^{b+1} \exp \{ -C_6 n^{1-2d_1} + n^a + C_7 n^b \} \right] \end{aligned}$$

for a positive constant C_6 and C_7 . This probability converges to zero as $n \rightarrow \infty$ when $0 < d_1 < \min \left(\frac{1-a}{2}, \frac{1-b}{2} \right)$.

S.5.7 Proof of Corollary 2

From Corollary 1 and Theorem 2,

$$\begin{aligned} & \mathbb{P}(\text{an error occurs in the PenPC algorithm}) \\ &= \mathbb{P}(\hat{\mathcal{C}}_{\mathcal{G}_n}(\boldsymbol{\theta}) \neq \mathcal{C}_{\mathcal{G}_n}) + \mathbb{P}(\hat{\mathcal{G}}_n^u(\alpha_n) \neq \mathcal{G}_n^u) \\ &= O(\exp\{2n^a - n^a \log(n)\}) + O(\exp\{-Cn^{1-2d_1}\}) \\ &= O(\exp\{-Cn^{1-2d_1}\}) \end{aligned}$$

for $d_1 < \min((1-a)/2, (1-b)/2)$.